

Determining F-theory matter via Gromov-Witten invariants

Amir-Kian Kashani-Poor^a

^b*LPENS, CNRS, PSL Research University, Sorbonne Universités, UPMC, 75005 Paris, France*

Abstract: We show how to use Gromov-Witten invariants to determine the matter content of F-theory compactifications on elliptically fibered Calabi-Yau manifolds X over Hirzebruch surfaces. To determine the representations of these matter multiplets under the gauge algebra \mathfrak{g} , we use toric methods to embed the weight lattice of \mathfrak{g} into the integer homology lattice of X . We then apply mirror symmetry to determine whether classes in this lattice corresponding to weights of given representations are represented by irreducible curves. Applying mirror symmetry efficiently to such geometries requires obtaining good approximations to their Mori cones. We show that whenever our approximations are smooth, they coincide with the Mori cone of X and already contain information on the matter content of compactifications on X . We finally study the different birationally equivalent geometries arising from our construction, and the flops relating them.

To Noah Kian, tenaciously, adorably, pursuing his sleep deprivation research agenda.

Contents

1	Introduction	4
2	F-theory matter via F-theory/M-theory duality	6
3	The geometries and their curves	8
3.1	Anti-canonical hypersurfaces in projective bundles over Hirzebruch surfaces .	8
3.2	Desingularization	10
3.3	Enhancing the singularity (before desingularizing anew)	12
3.4	$h^{1,1}(X)$	13
3.5	The sets $(\mathfrak{g})_n$ of birational equivalence classes	14
3.6	The Mori cone	17
3.7	Constructing torus invariant curves in the Mori cone of X	19
3.7.1	Type I: $u * v \in I_{Stanley-Reisner}$	21
3.7.2	Type II: $u * v \notin I_{Stanley-Reisner}$	24
3.8	Constructing Higgsing trees torically	26
4	Computing genus 0 Gromov-Witten invariants via mirror symmetry	28
4.1	Mirror symmetry for hypersurfaces in toric varieties: an algorithm for computing their Gromov-Witten invariants	30
4.1.1	A representative of Ω in appropriate coordinates on the complex structure moduli space $\mathcal{M}_{cplx}(X')$	31
4.1.2	The Picard-Fuchs system	32
4.1.3	A distinguished basis of periods at a MUM point	33
4.1.4	How to choose coordinates on complex structure moduli space – the prequel	34
4.1.5	Identifying the linear combinations of solutions which coincide with periods of Ω in a symplectic basis of $H_3(X', \mathbb{Z})$	35
4.2	How to choose coordinates on complex structure moduli space	35
4.3	The Gromov-Witten invariants of interest	36
4.4	Gromov-Witten invariants of birationally equivalent varieties	36
5	Identifying matter: the formalism applied	36
5.1	Embedding the root lattice $\Lambda^{root}(\mathfrak{g})$ in $N_1(X)$	37
5.2	Identifying matter	37
5.2.1	Complex vs. self-conjugate representations	37
5.2.2	When roots and weights coincide	38
5.2.3	Matter curves and the toric Mori cone	39
A	Assorted data on the birational equivalence classes $(\mathfrak{g})_n$	40
A.1	A-series	40

A.2	<i>B</i> -series	42
A.3	<i>D</i> -series	43
A.4	E_6	45
A.5	E_7	47
A.6	E_8	47
A.7	F_4	48
A.8	G_2	50

1 Introduction

String theory has an intimate connection to complex geometries that serve as supersymmetry preserving compactification manifolds. This relation is particularly elaborate in F-theory [1], where also the vacuum expectation value of the axio-dilaton is geometrized: it is identified with the complex structure modulus of a torus fibered over the compactification manifold. The understanding of F-theory compactifications on elliptic fibrations over Hirzebruch surfaces \mathbb{F}_n [2, 3] was substantially advanced in the seminal paper [4] in the context of heterotic/F-theory duality. In particular, it was found that while the gauge symmetry of the corresponding six dimensional theories follows easily from the Kodaira classification of the singularities of the elliptic fibration, the matter content is more difficult to extract from the geometry.

There has been a tremendous amount of work on F-theory compactifications on elliptically fibered geometries in the intervening twenty plus years. We touch upon a very few developments in the following few lines, and refer to the excellent recent review [5] for a more complete list of references. The geometries discussed in [4] were introduced in the context of toric geometry slightly earlier in [6]. Some observations made in that work regarding the interplay of toric data and the gauge symmetry of the compactification were explained in [7]. The question of identifying matter in F-theory compactifications, the topic of this paper, has received much attention, with some important developments being [8–10]. A decompactification limit of the Hirzebruch base of the compactification Calabi-Yau manifold yields six dimensional superconformal field theories. Interest in the study of these elusive theories was revived by classification proposals [11, 12], based on work classifying all bases appropriate for F-theory compactifications [13]. The observation that the elliptic genus of tensionless strings in these theories is captured by the topological string with target space the compactification manifold [14] has led to an improved understanding both of the tensionless strings that arise upon compactification of F-theory on elliptically fibered Calabi-Yau spaces [15–21] and on the topological string with such target spaces [22–25]. In particular, the connection has led to the computation of all genus modular results for the topological string partition function, order by order in base wrapping number.

In this work, we will put some of the enumerative invariants extracted from the topological string to work to determine the massless field content of 6d theories systematically and computationally effectively. We descend from the lofty heights of all genus results, as all we require are genus 0 invariants (though in the case of E-strings, these in fact uniquely specify all invariants [26]), which we obtain via mirror symmetry computations [27, 28].

The backbone of this work is the following. As we will review in section 2, determining the field content of an F-theory compactification on a geometry X requires knowledge of the curves C occurring in X and their intersection numbers with a set of divisors $\{D_i\}$ representing a basis of $H_4(X, \mathbb{Z})$. In section 3, we will construct X as a hypersurface in an

ambient toric variety Y . In particular, we will identify in subsection 3.7 the curves in X giving rise to vector multiplets associated to a gauge symmetry \mathfrak{g} in terms of intersections of X with torus invariant surfaces of Y . This will provide a map ϕ from the root lattice $\Lambda^{root}(\mathfrak{g})$ to the space N_1 spanned by classes of curves of X . We will then use mirror symmetry in section 4 to get a handle on all irreducible curves in X (up to a certain degree, depending on the computer time invested). Finally, extending ϕ over \mathbb{Q} to access the weight lattice $\Lambda^{weight}(\mathfrak{g})$, we will identify the representations \mathfrak{R}_i of all hypermultiplets present in the spectrum in section 5. In the appendix, we gather data regarding the various varieties that arise from the construction outlined in section 3.

While the focus of the paper is on extracting the matter content of F-theory compactifications from the Gromov-Witten invariants of the compactification manifold, we take the occasion in section 3 to discuss in detail the step from the initial toric fan yielding the ambient space for the Calabi-Yau hypersurface to the polytope from which the final fan, with required singularities imposed and resolved, can be extracted as a subdivision. We furthermore pay particular attention to the computation of the Mori cone of the Calabi-Yau hypersurface itself. Using an idea which goes back to Sheldon Katz, as cited in [29], we compute a better approximation to this cone, which we call the toric Mori cone, than that derived from the Mori cone of the ambient space. We use mirror symmetry to determine when the toric Mori cone coincides with the actual Mori cone of the Calabi-Yau manifold. We find, for the many examples that we consider, that this is the case whenever the toric Mori cone is smooth. The methods we employ also allow us to determine the different isomorphism classes of birationally equivalent varieties, related by flops, that occur when we impose a certain singularity over a Hirzebruch base \mathbb{F}_n . This lays the geometrical groundwork for extending the study in [30] of phases of five dimensional theories obtained from compactifying six dimensional theories on a circle beyond the maximally Higgsed case.

As the novelty in the mirror symmetry computations that we perform, compared e.g. to [16], is the use of the toric Mori cone, we review in detail in section 4 how the relation between the Mori cone (or an approximation thereof) of a Calabi-Yau manifold X and distinguished coordinates on the complex structure moduli space of its mirror X' arises, and we discuss how to proceed if the approximate Mori cone is not smooth.

For all things toric, we follow the notation of the wonderful book [31], where, unless otherwise noted, the proofs of all toric facts that we cite in this paper can be found. Extensive use of the mathematics software system SageMath [32] was made to perform the toric computations in this work. The mirror symmetry computations were performed in Mathematica [33]. The Mathematica package LieART [34] proved very useful for all computations involving Lie algebras and their representations.

As this paper was in the final phase of completion, we learned of the paper [35], which has some overlap with this work.

2 F-theory matter via F-theory/M-theory duality

In this section, we briefly review M-theory compactifications on Calabi-Yau manifolds X and how they related to F-theory compactifications on $X \times S^1$ when X is elliptically fibered [1]. These matters have recently been discussed in great detail in the review [5].

Perturbative gauge fields arise in M-theory compactifications on a Calabi-Yau manifold X via the expansion of the supergravity field C_3 in harmonic two forms,

$$C_3 = \sum_i A_i \omega^i. \quad (2.1)$$

Perturbative states are not charged under the gauge fields A_i . In particular, the perturbative gauge symmetry is abelian. Non-perturbatively, the story is much richer. C_3 is sourced electrically by M2 branes. This coupling is described by an interaction term

$$I_{int} = \int C_3 \quad (2.2)$$

on the worldvolume of M2 branes. An M2 brane wrapping a holomorphic curve C in X gives rise to a BPS multiplet of particles. Their worldline action contains the coupling

$$\int dt A_i \int_C \omega^i = C \cdot D^i \int dt A_i, \quad (2.3)$$

where we have introduced divisors D_i , representatives of the Poincaré dual homology class in $H_4(X, \mathbb{Z})$ to the cohomology classes $[\omega_i]$. From (2.3), we can read off the charge of these particles under the gauge field A_i : it is given by the intersection product $C \cdot D^i$. The spins of these particles depend on the moduli space of the M2 brane: an isolated curve gives rise to a hypermultiplet, a curve with a genus g Riemann surface as moduli space gives rise to a vector multiplet and $2g$ hypermultiplets [36, 37].

M-theory on an elliptically fibered Calabi-Yau manifold X is dual to F-theory on $X \times S^1$. The elliptic fiber of X becomes fully physical in the M-theory picture; its size maps to the inverse radius of the S^1 in the F-theory frame. The 5d theory obtained by compactification of M-theory on X lifts to a 6d theory by mapping to the F-theory picture and decompactifying the S^1 . In this paper, we will be interested in particular in vector fields that lift to 6d vector fields (rather than lifting to a component of the metric or a tensor field). Aside from the perturbative vector fields introduced in (2.1), M2 branes wrapping curves C which arise from resolving singularities in the elliptic fiber of X give rise to such vector fields. The associated vector multiplets are charged under a subset $\{A_i\}_{i \in J}$ of the perturbative gauge fields. This mechanism results in enhanced gauge symmetry with gauge group of rank $|J|$ at the singular point of the geometry.

To pinpoint the Lie algebra \mathfrak{g} underlying the gauge symmetry, we identify the A_i with the

Cartan generators H_{α_i} of \mathfrak{g} in the Chevalley basis. Recall that in this basis, Cartan generators are labeled by simple roots α_i ($\alpha_i \in \Delta$), and completed to a basis of \mathfrak{g} via elements E_α labeled by the roots α ($\alpha \in \Phi$) (matching the count $\dim \mathfrak{g} = |\Phi| + |\Delta|$). The structure constants of the Lie algebra are then determined by the bilinear form (\cdot, \cdot) induced on Φ via the Killing form of \mathfrak{g} as

$$[H_{\alpha_i}, E_\alpha] = (\alpha, \alpha_i^\vee) E_\alpha = \alpha(H_{\alpha_i}) E_\alpha. \quad (2.4)$$

A curve C giving rise to a BPS multiplet containing the vector field associated to the Lie algebra generator E_α thus must exhibit intersection numbers with the divisors D^i corresponding to the negative of the i^{th} coefficient of the root α in an expansion in fundamental weights,¹

$$C \cdot D^i = -\alpha(H_{\alpha_i}). \quad (2.5)$$

Note that the charge of a field associated to a curve C is fixed entirely by its homology class (or more precisely by its class in the space N_1 , which we introduce in section 3.6 below). Conversely, in order for a field with the charges associated to a given homology class to be part of the spectrum of the theory compactified on X , that class must be represented by an irreducible curve.

Isolated curves in the fiber will give rise to fields belonging to charged hypermultiplets, transforming in a representation \mathfrak{R} of \mathfrak{g} . We will call such curves *matter curves*. To each $\lambda \in \Pi(\mathfrak{R})$, $\Pi(\mathfrak{R})$ denoting the set of weights associated to \mathfrak{R} , are associated one or multiple basis vectors of the representation space $V_{\mathfrak{R}}$. The charges of the corresponding fields under the gauge fields A_i are given by $\lambda(H_{\alpha_i})$. A curve C giving rise to such a multiplet must hence exhibit intersection numbers satisfying

$$C \cdot D^i = -\lambda(H_{\alpha_i}). \quad (2.6)$$

Determining the field content of an F-theory compactification on a geometry X therefore requires knowledge of the irreducible curves C occurring in X and their intersection numbers with a set of divisors $\{D_i\}$ representing a basis of $H_4(X, \mathbb{Z})$. We turn to these questions in the following section.

¹That a minus sign must be present in (2.5) is perhaps clearest in the case of elliptic surfaces, where rational curves C with $C \cdot C = -2$ map to simple roots α with $\alpha(H_\alpha) = 2$.

3 The geometries and their curves

3.1 Anti-canonical hypersurfaces in projective bundles over Hirzebruch surfaces

The starting point of our considerations is the projective bundle $Y_{\Sigma_n} = \mathbb{P}^{2,3,1}(2\mathcal{K}_{\mathbb{F}_n} \oplus 3\mathcal{K}_{\mathbb{F}_n} \oplus \mathcal{O})$ over a Hirzebruch surface \mathbb{F}_n . $\mathcal{K}_{\mathbb{F}_n}$ here indicates the canonical line bundle of \mathbb{F}_n , and we follow the convention that $\mathbb{P}(\mathcal{E})$ indicates the projectivization of the dual bundle $-\mathcal{E}$. The total space of the projective bundle is a (singular) toric variety. The notation indicates that this geometry is associated to the toric fan Σ_n . For brevity, we will also write Y_n . The generators u_ρ of the 1-cones $\rho \in \Sigma_n(1)$ of this geometry are given in table 3.1.

					$(\mathbb{C}^*)_1$	$(\mathbb{C}^*)_2$	$(\mathbb{C}^*)_3$
u_{ρ_x}	1	0	0	0	2	0	0
u_{ρ_y}	0	1	0	0	3	0	0
u_{ρ_z}	-2	-3	0	0	1	$n-2$	-2
u_{ρ_s}	-2	-3	0	-1	0	$-n$	1
u_{ρ_t}	-2	-3	0	1	0	0	1
u_{ρ_u}	-2	-3	-1	$-n$	0	1	0
u_{ρ_v}	-2	-3	1	0	0	1	0

Table 3.1: Toric data for $\mathbb{P}^{2,3,1}(2\mathcal{K}_{\mathbb{F}_n} \oplus 3\mathcal{K}_{\mathbb{F}_n} \oplus \mathcal{O}) \rightarrow \mathbb{F}_n$.

Recall that one useful way of thinking about toric varieties associated to a fan Σ is in terms of the homogeneous coordinate ring (or Cox ring) [38, 39]: each 1-cone generator u_{ρ_i} is assigned a \mathbb{C} valued coordinate x_i , called a homogeneous coordinate. Coordinates whose associated 1-cone generators do not jointly belong to any cone in the fan cannot vanish simultaneously. The monomials formed from the products of the elements of each such set generate the so-called Stanley-Reisner ideal $I_{\text{Stanley-Reisner}}$, with vanishing locus Z . The toric variety is obtained as the quotient

$$Y_\Sigma = (\mathbb{C}^{|\Sigma(1)|} - Z)/G, \quad (3.1)$$

with $G \cong (\mathbb{C}^*)^{|\Sigma(1)|-d}$ the group of relations among the 1-cone generators.

In table 3.1, we give a set of generators for the group G of relations of the toric variety Y_{Σ_n} . Note that we have indexed the rays $\rho \in \Sigma(1)$ by the variables we shall assign to them.

The bundle Y_{Σ_n} is chosen such that the generic section of the anti-canonical bundle $-\mathcal{K}_{Y_n}$ of its total space defines an elliptically fibered Calabi-Yau manifold.² A basis for $\Gamma(Y, -\mathcal{K}_{Y_n})$,

²Note that as Y_{Σ_n} is singular, we need to argue that it is Gorenstein such that its dualizing sheaf is indeed a line bundle. We will do so in section 3.2.

the vector space of global holomorphic sections of $-\mathcal{K}_{Y_n}$, can be obtained from the polyhedron

$$P_{-K_{Y_n}} = \{m \in M_{\mathbb{R}} \mid \langle m, u_{\rho} \rangle \geq -1 \ \forall \rho \in \Sigma(1)\}. \quad (3.2)$$

To see this, recall that to any torus invariant Weil divisor $D = \sum_{\rho} a_{\rho} D_{\rho}$, we can associate the polyhedron

$$P_D = \{m \in M_{\mathbb{R}} \mid \langle m, u_{\rho} \rangle \geq -a_{\rho} \ \forall \rho \in \Sigma(1)\}. \quad (3.3)$$

We obtain (3.2) by noting that the anti-canonical divisor of a toric variety is given by $-K = \sum D_{\rho}$. In general, the lattice M can be identified with the lattice of characters of the torus $T \subset Y$ underlying the toric variety Y . We write χ^m for the character associated to $m \in M$. Its dual lattice N coincides with the lattice of one-parameter subgroups of T . The elements of the lattice M lying in the intersection with $P_{-K_{Y_n}}$ yield the desired basis:

$$\Gamma(Y, -\mathcal{K}_{Y_n}) = \bigoplus_{m \in P_{-K_Y} \cap M} \mathbb{C} \cdot \chi^m. \quad (3.4)$$

Upon choosing a basis $\mathbf{t} = (t_1, \dots, t_4)$ for T , this becomes $\chi^m = \prod t_i^{(m)_i}$. We will use the notation

$$L(P_{-K_Y}) \quad (3.5)$$

for $\Gamma(Y, -\mathcal{K}_{Y_n})$ expressed in this basis.

In homogeneous coordinates, the characters χ^m are given by

$$\chi^m \Rightarrow \prod_{\rho} x_{\rho}^{\langle m, u_{\rho} \rangle + 1}, \quad (3.6)$$

the specialization of the general relation $\chi^m \Rightarrow \prod_{\rho} x_{\rho}^{\langle m, u_{\rho} \rangle + a_{\rho}}$ to the anti-canonical bundle.

It now follows from the 1-cone generators given in table 3.1 that a general section of $-\mathcal{K}_{Y_n}$ in homogeneous coordinates is of the form

$$s_{-\mathcal{K}_{Y_n}} = \alpha y^2 + a_1 x y z + a_3 y z^3 - (\beta x^3 + a_2 x^2 z^2 + a_4 x z^4 + a_6 z^6), \quad (3.7)$$

with the coefficients a_i functions of the remaining coordinates u, v, s, t . α and β are constants that can be absorbed in the coordinates x and y . The minus sign is to match the conventions of [4]. The anti-canonical hypersurface X_n of Y_n given by

$$X_n = \{p \in Y_n \mid s_{-\mathcal{K}_{Y_n}}(p) = 0\} \quad (3.8)$$

is the central object of interest in this paper. It is Calabi-Yau by construction. From (3.7), it is evident that it is given by an elliptic fibration over the Hirzebruch base \mathbb{F}_n . This fibration will generically be singular at $y = s = 0$. The vanishing degree n_i in the variable s of the

coefficients a_i determines the singularity type of the elliptic fiber over the corresponding points of the base surface \mathbb{F}_n .

Note that in the patch $z = 0$, the equation $s_{-\mathcal{K}_{Y_n}} = 0$ has a unique solution $(x : y : z) \sim (1 : \sqrt{\frac{\beta}{\alpha}} : 0)$ (the two points corresponding to the two signs of the square root are identified by the weighted projective action) which is independent of the coordinates on \mathbb{F}_n . This defines a global holomorphic section (called the zero section) of the elliptic fibration, allowing the embedding of the base \mathbb{F}_n into X_n . We will call the image of this section Z . The point in each fiber defined by the intersection with the divisor $z = 0$ yields the distinguished point (the zero element of the additive group) of the elliptic fiber.

3.2 Desingularization

The strategy for desingularizing X_n will be to find a Y'_n birationally equivalent to the ambient space Y_n , $\phi : Y'_n \rightarrow Y_n$, such that $\phi^{-1}X_n$ is smooth. Note that ϕ is generically not a resolution of singularities of Y_n . In fact, our considerations here can equally well be applied to the projective bundle $\mathbb{P}^{1,1,1}(2\mathcal{K}_{\mathbb{F}_n} \oplus 3\mathcal{K}_{\mathbb{F}_n} \oplus \mathcal{O})$, which is smooth. The procedure we will review [40] relies on constructing a Y'_n which is a Gorenstein orbifold with terminal singularities (we will explain the term ‘Gorenstein’ and how to diagnose terminal singularities in the toric setting in the ensuing discussion). It can be shown that the generic zero section of a base-point free line bundle on such spaces share all three properties, at least in the case of toroidal singularities (see theorem 2.6 and proposition 4.3 of [41]).³ As Gorenstein orbifolds with terminal singularities have singularities in codimension 4 and higher, the three dimensional anti-canonical hypersurfaces in Y'_n that will be the objects of our interest will be smooth. We will drop the subscript n for the rest of the discussion in this subsection.

As we are considering toric orbifolds Y' , i.e. ambient spaces that are generically not smooth, it is not guaranteed that their anti-canonical divisor is Cartier, hence describes a line bundle over Y' . Y' is called Gorenstein when this is the case. There is a simple criterion for when a toric Weil divisor is Cartier: the polyhedron (3.3) must be a lattice polytope. A Gorenstein variety is hence characterized by the fact that the polyhedron P_{-K_Y} defined in (3.2) be a lattice polytope.

Via the correspondence

$$\begin{aligned} \{(Y_\Sigma, D) \mid \Sigma \text{ a complete fan in } N_{\mathbb{R}}, D \text{ a torus invariant ample divisor on } Y_\Sigma\} \\ \Downarrow \\ \{\text{lattice polytopes } P \subset M_{\mathbb{R}}\} \end{aligned}$$

we can recover a fan Σ_P together with an ample line bundle D on X_{Σ_P} from a lattice

³Thanks to Antonella Grassi for requesting a reference, and to Andrew Harder for providing one.

polytope. If P is defined via (3.2), then Σ_P does not generically coincide with the fan Σ that we started with. It is obtained as the normal fan to the lattice polytope P , of which Σ is a refinement. By the toric Kleiman criterion, ampleness of a Cartier divisor D is equivalent to positivity of all intersections of D with torus invariant irreducible curves C , $D \cdot C > 0$. In the process of refinement, the anti-canonical line bundle can lose its ampleness property. The weaker property of base-point freeness however depends only on the polytope, hence holds for the anti-canonical line bundle of all subdivisions of P .

A lattice polytope of the form (3.2) is called reflexive. Its unique interior lattice point is the origin. The concept of dual (or polar) polytopes is particularly useful in the case of reflexive polytopes. The general definition

$$P^\circ = \{u \in N_{\mathbb{R}} \mid \langle m, u \rangle \geq -1 \ \forall m \in P\} \quad (3.9)$$

applied to the polytope P with facet presentation

$$P = \{m \in M_{\mathbb{R}} \mid \langle m, u_F \rangle \geq -a_F \ \text{for all facets } F\}, \quad (3.10)$$

all $a_F > 0$, yields

$$P^\circ = \text{Conv}\left(\frac{1}{a_F} u_F \mid F \text{ a facet of } P\right). \quad (3.11)$$

As facet normals u_F are lattice vectors of N by definition, it follows easily that the dual of a reflexive polytope is again a lattice polytope. It is in fact also reflexive. The normal fan of P is the face fan of P° and vice versa.

As singularities are local properties of a variety, we can study them by considering the variety patch by patch. Given an affine patch U_σ associated to a cone $\sigma \in \Sigma$ of a fan, we can determine the type of singularities it contains by considering the lattice points contained in the polytope

$$P_\sigma = \text{Conv}(0, u_\rho \mid \rho \in \sigma(1)) \quad (3.12)$$

given by the convex hull of the origin and the tips of the 1-cone generators u_ρ of σ . Indeed, if all the u_ρ lie on a hyperplane at a distance 1 from the origin, i.e.

$$\exists m \in M : \langle m, u_\rho \rangle = 1 \quad \forall \rho \in \sigma(1), \quad (3.13)$$

then U_σ has terminal singularities iff the only lattice points of P_σ are given by its vertices.

It is now clear that to obtain a fan Σ , with $\Sigma(1) \supset \Sigma_P(1)$, whose associated toric variety has terminal singularities, we must introduce additional 1-cones through all lattice points $P^\circ \cap N$. This leads to the following definition [40, 42]: a maximal projective subdivision of a reflexive polytope P is a regular simplicial fan Σ such that $\Sigma(1) = \{\langle u_\rho \rangle \mid u_\rho \in P^\circ \cap N\}$. Simplicial fans lead to toric varieties with at worst orbifold singularities. For smooth fans,

regularity ensures that the corresponding toric variety is projective. Note that in [42], maximal projective subdivisions are required to refine the normal fan of P . We will not do so, as subdivisions which do not refine the normal fan will also prove of interest to us.

Consider now a maximal projective subdivision Σ of P . As Σ is simplicial by definition, X_Σ is an orbifold. The polyhedron associated to the anti-canonical divisor of X_Σ is the lattice polytope P , hence X_Σ is Gorenstein and its anti-canonical bundle is base-point free. As P° has the origin as unique interior point and by maximality of the subdivision, all patches U_σ of Σ have terminal singularities. We thus conclude that X_Σ is a Gorenstein orbifold with terminal singularities.

Let us now relate this discussion to the fans Σ_n introduced in section 3.1. To use maximal projective subdivisions of the dual polytope to desingularize X_n , two conditions need to be met:

1. $P_{-K_{Y_n}}$ must be a lattice polytope, thus reflexive. This is the case for $n = 0, 1, 2, 3, 4, 6, 12$. By the above, this is the statement that for these values of n , a birationally equivalent geometry to Y_n exists, given by the normal fan to $P_{-K_{Y_n}}$, that is Fano, i.e. whose anti-canonical bundle is ample. We will discuss how to treat some other values of n below.
2. For $P_{-K_{Y_n}}$ reflexive, any maximal projective subdivision Σ' satisfies

$$\Sigma_n(1) \subset \Sigma'(1). \quad (3.14)$$

However, as already mentioned above, the subdivisions need not be refinements of Σ_n . In fact, for $n = 3$ (and only for this value among the 7 for which $P_{-K_{Y_n}}$ is reflexive), none of the maximal projective subdivisions of $P_{-K_{Y_n}}$ refine Σ_3 . In section 3.7.2, we will see that they nevertheless give rise to the expected gauge symmetry upon F-theory compactification.

3.3 Enhancing the singularity (before desingularizing anew)

The discussion up to this point was concerned with the resolution of the generic singularity of an anti-canonical section of Y_n . In the local context, these give rise to the maximally Higgsed theories discussed in [43]. To enhance the singularities of the anti-canonical section (3.7), and thus unHiggs the gauge symmetry of the F-theory compactification, we need to define a lattice polytope P_{sing} in M defined by excluding those points of P_{-K_Y} which map to sections with a vanishing degree in s too low for the singularity desired. To define P_{sing} , first determine the subset S_{sing} of $P_{-K_Y} \cap M$ corresponding to all sections compatible with the singularity. Next, define the polyhedron

$$P_{aux} = \{u \in N_{\mathbb{R}} \mid \langle m, u \rangle \geq -1 \ \forall m \in S_{sing}\}. \quad (3.15)$$

S_{sing} needs to be sufficiently rich, i.e. the constraints on the vanishing degrees in s sufficiently lax, for P_{aux} to be a compact polyhedron. Its dual is then the lattice polytope we are after,

$$P_{sing} = P_{aux}^\circ = \{m \in M_{\mathbb{R}} \mid \langle m, u \rangle \geq -1 \ \forall u \in P_{aux}\}. \quad (3.16)$$

To argue that the polyhedron P_{sing} is a lattice polytope, and hence reflexive, note that a selection $\{m_F\}$ among the elements of S_{sing} is possible such that

$$P_{aux} = \{u \in N_{\mathbb{R}} \mid \langle m_F, u \rangle \geq -1 \text{ for all facets } F \text{ of } P_{aux}\}. \quad (3.17)$$

By the discussion around (3.11), the dual of P_{aux} is given by the convex hull of the facet normals m_F of P_{aux} , is hence a lattice polytope.

Clearly, $S_{sing} \subset P_{sing}$. If $S_{sing} \neq P_{sing} \cap M$, the points of S_{sing} cannot be described as all lattice points of a lattice polytope, and the singularity desired cannot be realized torically over the given base.

If we apply these considerations to the set $S_{sing} = P_n \cap M$ with P_n the lattice polytopes defined in the previous subsection, then the polytope P_{sing} we obtain is the smallest reflexive polytope containing S_{sing} . For all n for which P_n is a lattice polytope (recall that these are $n = 0, \dots, 4$ and $n = 6, 12$), it coincides with P_n . If $P_{sing} \neq P_n$ but n is in the range $0 \leq n \leq 12$, P_{sing} can replace P_n as the starting point of the desingularization process described in subsection 3.2. Beyond $n = 12$, P_{sing} is non-compact for any choice of singularity.

In some cases, merely studying the vanishing orders of sections in the variable s can be misleading, as variable definitions are possible which increase some vanishing orders (cf. the discussion of split, semi-split, and non-split singularities in [4], to which we will return in section 3.8). In such cases, computing $h^{1,1}(X)$ of the resolved geometry can serve as an indication for which singularity among the two or three possibilities was realized before desingularization.

3.4 $h^{1,1}(X)$

Mirror symmetry requires knowledge of the Kähler cone of the anti-canonical hypersurface $X \subset Y$. This will be the topic of subsection 3.6. A cruder question is that of the $2d - 2$ homology. For the ambient space Y , given by a maximal projective subdivision Σ of the lattice polytope P , this space is generated by the classes of torus invariant divisors under linear equivalence, hence

$$h^{1,1}(Y) = |\Sigma(1)| - 4. \quad (3.18)$$

The intersections of the toric divisors of Y with the anti-canonical hypersurface X are either empty or yield reducible or irreducible divisors of X . It can be shown [40] that a divisor

generically misses X iff the corresponding cone generator lies on a facet of P° . Such divisors will thus be of no interest to us in the following and the corresponding 1-cones will be discarded (rendering the ambient spaces obtained from triangulations of the retained 1-cones more singular). The divisors that potentially lead to reducible intersections are those which lie in the interior of codimension 2-faces Θ° of P° . The number of irreducible components of such intersections is captured by the number of interior points of the dual face to Θ° , the 1-face Θ of P . Introducing the notation $l^*(\Theta)$ for the number of interior points lying on a face Θ , the number of irreducible components of the intersection $D \cap X$ for a divisor D whose associated 1-cone generators lies on a codimension 2 face θ of P° is given by $l^*(\Theta) + 1$. This yields the following expression for the (1,1) Hodge number of X :

$$h^{1,1}(X) = |\Sigma(1)| - 4 - \sum_{\Gamma^\circ \in F_1(P^\circ)} l^*(\Gamma^\circ) + \sum_{\Theta^\circ \in F_2(P^\circ)} l^*(\Theta^\circ)l^*(\Theta), \quad (3.19)$$

where we have introduced the notation $F_n(P)$ for the set of codimension n faces of the polytope P .

To have toric methods capture the geometry of the variety X as accurately as possible, we will hence need to describe it as an anti-canonical hypersurface in a toric ambient space with fan Σ which maximizes

$$|\Sigma(1)| - 4 - \sum_{\Gamma^\circ \in F_1(P^\circ)} l^*(\Gamma^\circ), \quad (3.20)$$

thus reducing the correction term. We conclude that the construction from section 3.3 can be useful even for $S_{sing} = P_n \cap M$: the polytopes P_{sing} we construct in these cases contain the same interior points as P_n . As they are the smallest lattice polytopes to contain these points, they will generically have more facets than P_n , thus have duals P° with more vertices, leading to a maximization of (3.20). It can happen however that even upon considering these smallest polytopes, the intersection of some divisors of Y with X is reducible. We discuss this further in subsection 3.8 in the context of constructing Higgsing trees.

3.5 The sets $(\mathfrak{g})_n$ of birational equivalence classes

A refinement of a fan $\Sigma' \rightarrow \Sigma$ yields a proper birational toric morphism $Y_{\Sigma'} \rightarrow Y_\Sigma$ between the associated toric varieties. All maximal projective subdivisions of P which are refinements of the normal fan of P hence lead to birational varieties. A result of the toric minimal model program is that all such geometries are related by a sequence of flops. In three dimensions, a toric flop is easily visualized, see figure 1: four generically positioned 1-cones can be triangulated in two ways to yield two maximal dimensional cones. To argue for this intuitive fact (the higher dimensional analogue will be less so), note that a fine triangulation involving four generically positioned 1-cones will contain exactly two 3-cones, and these will intersect in a 2-cone, which we will call a wall. The choice of wall uniquely fixes the

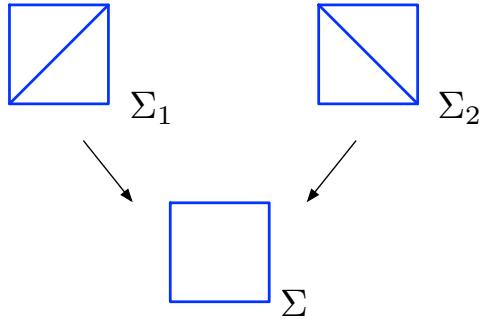
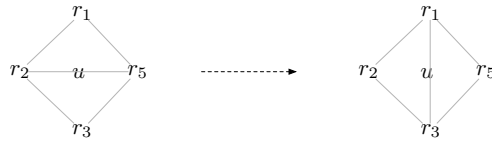


Figure 1: A toric flop in three dimensions.

triangulation. The question hence reduces to that of determining the maximal number of walls. The defining property of the two 1-cones spanning the wall is that the hyperplane containing them, assuming genericity, divides the lattice N into two disconnected regions, each of which contains exactly one of the two remaining 1-cones. It is now evident that exactly two such configurations exist. In four dimensions, a hyperplane is spanned by three 1-cones, hence the walls associated to any two distinct triangulations of five 1-cones will have one 1-cone in common. We can depict such configurations by writing the four cones involved in the following configuration:



The central 1-cone (with generator ρ_u in the above example) is the one the two walls have in common. The outer 1-cones along the horizontal respectively vertical axis (with generators ρ_{r_2}, ρ_{r_5} and ρ_{r_1}, ρ_{r_3} respectively in the above example) are those which lie in separate 4-cones in one or the other triangulation.

Two four dimensional varieties whose fans differ by a flop are equal outside a locus of codimension at least 2. The corresponding anti-canonical hypersurfaces of two merely birational varieties are hence isomorphic if this locus does not intersect the hypersurfaces.

In our study of anti-canonical hypersurfaces, we will thus identify all maximal projective subdivisions of P which differ only in a locus which does not intersect the associated anti-canonical hypersurface. We find that the number of isomorphism classes among the hypersurfaces X is far few than the corresponding number for the ambient space Y . E.g., all polytopes associated to an E_6 singularity over \mathbb{F}_n exhibit 200 maximal projective subdivisions, but merely four (for n even) or eight (for n odd) isomorphism classes of hypersurfaces. We will denote the set of all isomorphism classes of hypersurfaces associated to a given singularity \mathfrak{g} over the base \mathbb{F}_n as $(\mathfrak{g})_n$. These classes correspond to birationally equivalent

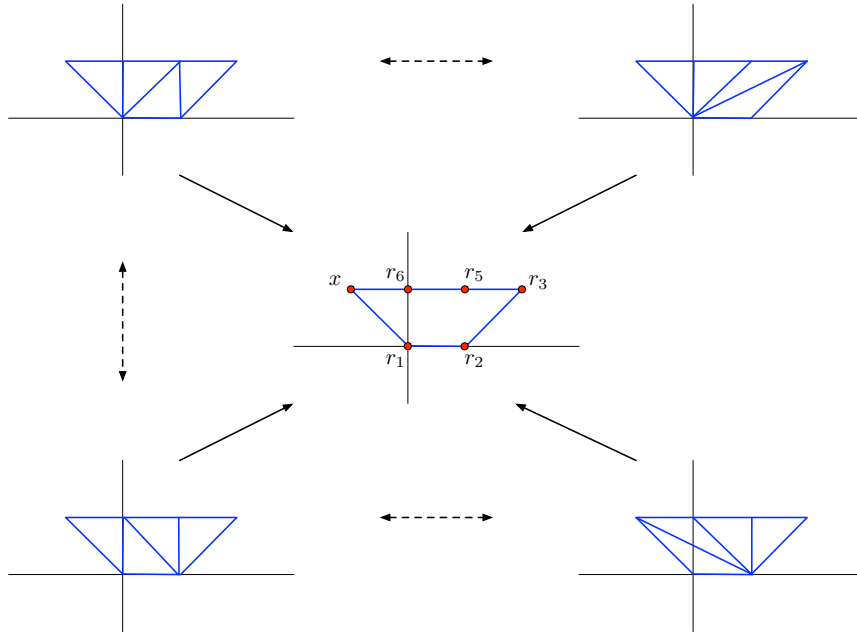


Figure 2: All flops relating $(E_6)_n$ varieties of embedding type I.

varieties, disregarding the embedding into the ambient space. We will refer to the elements of $(\mathfrak{g})_n$ as $(\mathfrak{g})_n$ varieties.

$(\mathfrak{g})_n$ varieties can be divided into two (not necessarily non-empty) disjoint sets, the elements of which we will refer to as *of embedding type I* and *of embedding type II*. Elements within each set are related via flops along curves contained in the fiber of the elliptic fibration. When both sets are non-empty, pairs containing an element from within each set exist which are related by a flop along a curve which involves the base of the Hirzebruch surface. Starting from a hypersurface fibered over \mathbb{F}_n , flopping with regard to a curve involving the base curve of \mathbb{F}_n introduce a 4-cone which contains both ρ_u and ρ_v among their generators. The monomial $u * v$ is hence removed from the Stanley-Reisner ideal, which implies that the base \mathbb{P}^1 is disrupted. These flops destroy the original fibration structure of the ambient space Y_n that we started with.

$(A_2)_3$ is the only non-empty class containing no variety of embedding type I, whereas varieties of embedding type II arise exactly for those odd n for which $(\mathfrak{g})_n$ is not empty.

Example: $(E_6)_n$ All $(E_6)_n$ Calabi-Yau hypersurface families for $n = 1, \dots, 5$ exhibit four isomorphism classes of embedding type I. These can be related by a sequence of flops which, at the level of the ambient space, involve flopping two 3-cones, always with ρ_u and ρ_v featuring as the central nodes. Dropping the central node, all involved 1-cone generators end on a common 2-plane, as depicted in figure 2. In more detail, the flop relating the top two partial fans in figure 2 is given in figure 3.

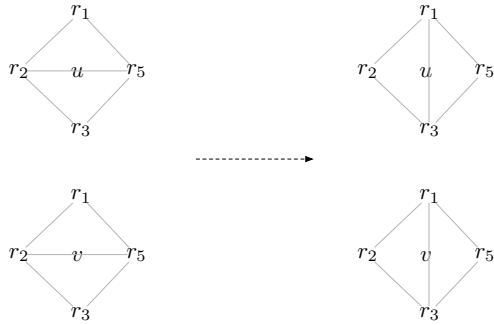


Figure 3: The top flop in figure 2 in detail.

3.6 The Mori cone

By the discussion in section 2, BPS states in M-theory compactified on a Calabi-Yau manifold X arise from M2 branes wrapping curves in X . The charges of the associated states arise from the intersection numbers of these curves with divisors of X . A first step in studying these curves will hence consist in studying them modulo numerical equivalence \equiv (i.e. identifying curves that have identical intersection numbers with all divisors). The free abelian group generated by the classes of irreducible complete curves⁴ under \equiv is denoted as $N_1(X)$. The cone within $N_1(X)$ generated by these classes is called $\text{NE}(X)$. Its closure, $\overline{\text{NE}}(X)$, is called the Mori cone and will play an important role in the following: this is where the representatives of curves we wish to identify sit.

The Mori cone of the complete toric ambient space Y with at worst orbifold singularities (i.e. with simplicial fan Σ_Y) is easy to determine, as it is spanned by the classes of torus invariant curves. The latter are in one-to-one relation to $n - 1$ cones τ of Σ_Y , and correspondingly denoted as $V(\tau)$. For Y complete, such τ always are the intersection of two n cones σ_1 and σ_2 , $\tau = \sigma_1 \cap \sigma_2$. We called such $n - 1$ cones walls above. We will call the tuple of intersection numbers of such a curve with all torus invariant divisors D_ρ (corresponding to 1-cones ρ of Σ_Y) the (toric) Mori vector of the curve. Its entries are computed as follows:

1. If $\rho \notin \sigma(1)$ for either $\sigma \in \{\sigma_1, \sigma_2\}$, the intersection number is zero.
2. If $\rho = \sigma(1) - \tau(1)$ for one $\sigma \in \{\sigma_1, \sigma_2\}$, the intersection number is

$$D_\rho \cdot V(\tau) = \frac{\text{mult}(\tau)}{\text{mult}(\sigma)}, \quad (3.21)$$

where the multiplicity of a cone is a measure of how singular it is. For smooth cones, the multiplicity is one.

3. If $\rho \in \tau(1)$, invariance of the intersection number under linear equivalence can be used

⁴We use the algebraic geometric language; for those more familiar with the analytic setting, ‘complete’ can be replaced with ‘compact’ in the following, with little loss of precision.

to choose a representative of the class $[D_\rho]$ that does not involve $D_{\rho'}$ for any $\rho' \in \tau(1)$. The intersection product of D_ρ with $V(\tau)$ can then be evaluated term by term by invoking 1. and 2.

We can sidestep the above procedure and obtain the intersection number $D_\rho \cdot V(\tau)$ for all $\rho \in \Sigma(1)$ in one go via the following observation. Any character χ^m for $m \in M$ defines a principal divisor, which can be decomposed in terms of the torus invariant divisors D_ρ as

$$0 \sim (\chi^m) = \sum_{\rho \in \Sigma(1)} \langle m, u_\rho \rangle D_\rho. \quad (3.22)$$

Considering the intersection number with a curve C yields

$$\forall m \in M : \quad 0 = \langle m, \sum_{\rho \in \Sigma(1)} (C \cdot D_\rho) u_\rho \rangle \quad \Rightarrow \quad \sum_{\rho \in \Sigma(1)} (C \cdot D_\rho) u_\rho = 0. \quad (3.23)$$

Equation (3.23) implies that Mori vectors encode relations between the cone generators u_ρ . From the discussion of intersection numbers, we know that the only non-vanishing coefficients arise for $\rho \in \sigma_1(1) \cup \sigma_2(1)$. Thus, by normalizing the coefficients of the relation among these $n + 1$ cone generators, e.g. by using (3.21), we obtain the Mori vector of the curve C . It is a theorem (best proved by considering the dual of the Mori cone, which we shall discuss momentarily) that the Mori cone of Y is spanned by the Mori vectors of the torus invariant curves $V(\tau)$. Our discussion of the computation of the Mori cone of Y is therefore complete.

The computation of the Mori cone of the Calabi-Yau hypersurface X is substantially more difficult. Note that the curves on Y generically intersect X in points or not at all. It would hence seem that $\overline{\text{NE}}(Y)$ contains little information with regard to $\overline{\text{NE}}(X)$. To see that this is not the case, we introduce the dual cone to the Mori cone, the so-called Nef cone. The Nef cone sits inside N^1 , the abelian group generated by Cartier divisors up to numerical equivalence. Modding out by numerical equivalence to define both N_1 and N^1 guarantees that the intersection product defines a non-degenerate pairing between these two spaces, and allows for the definition $\text{Nef} = \overline{\text{NE}}^\vee$. From the definition of $\overline{\text{NE}}$, we see that the Nef cone is spanned by Cartier divisor classes $[D]$ that satisfy $D \cdot C \geq 0$ for all complete irreducible curves C (indeed, such Cartier divisors are called **numerically effective**). Dealing with divisors rather than curves has the advantage that the non-empty intersections of divisors of Y with X yield (not necessarily irreducible) divisors of X . Indeed,

$$\text{Nef}(Y)|_X \subset \text{Nef}(X). \quad (3.24)$$

While the torus invariant divisors of Y are in one-to-one relation with the elements of $\Sigma(1)$, the Nef condition depends on how these 1-cones are assembled into fans.

As we discussed in section 3.5, many different maximal projective subdivisions of P can lead

to the same hypersurface X . We hence obtain a better approximation of the Nef cone of X than the inclusion (3.24) by considering

$$\bigcup_{\substack{\{\text{maximal projective} \\ \text{subdivisions } \Sigma \text{ of } P \\ \text{yielding isomorphic } X\}}} \text{Nef}(Y_\Sigma)|_X \subset \text{Nef}(X). \quad (3.25)$$

The dual of this relation,

$$\bigcap_{\substack{\{\text{maximal projective} \\ \text{subdivisions } \Sigma \text{ of } P \\ \text{yielding isomorphic } X\}}} (\text{Nef}(Y_\Sigma)|_X)^\vee \supset \overline{\text{NE}}(X), \quad (3.26)$$

allows us to determine an approximation to the Mori cone of X . We will refer to the cone defined in (3.25) as *the toric Kähler cone*, and the cone in (3.26) as *the toric Mori cone*.

Once we have computed the Gromov-Witten invariants for X , we can determine whether the toric Mori cone coincides with $\overline{\text{NE}}(X)$ by determining the Gromov-Witten invariants of its generators. If an invariant is non-vanishing, we can conclude that the corresponding class is represented by a curve in X . As $\overline{\text{NE}}(X)$ is contained in the toric Mori cone, all generators of the latter having non-vanishing invariants suffices to conclude that the two coincide. In practice, we have found that this is the case whenever the toric Mori cone is smooth.

Example: $(E_6)_3$ The generators of the toric Mori cone of one of the four $(E_6)_3$ varieties of embedding type I (in the terminology introduced in section 3.5) are given in table 3.2. $(E_6)_n$ for $n = 1, \dots, 5$ each contain a variety with nearly identical Mori cone, differing only in the last generator C_9 . This is also true for the other three embedding type I varieties in $(E_6)_3$. Upon providing a useful basis of torus invariant curves in the next subsection, we will return to this example and the interpretation of the generators in section 3.7.1.

3.7 Constructing torus invariant curves in the Mori cone of X

Distinguished curve and divisor classes in elliptically fibered Calabi-Yau manifolds X in the context of F-theory models have been discussed in [44–46] and reviewed in the recent lecture notes [5]. Aside from the embedding of the base and fiber curve of the Hirzebruch surface \mathbb{F}_n into X via the zero section of the fibration, called C_B and C_F below, the curves of interest are fibral curves: the generic elliptic fiber C_E , the rational curves C_{r_i} , $i \in 1, \dots, \text{rk}(\mathfrak{g})$, resolving the singularities of X , and the rational curve C_{r_0} . Unlike the C_{r_i} , $i > 0$, C_{r_0} intersects the zero section. The curve classes $[C_E]$, $[C_{r_0}]$ and $[C_{r_i}]$ are related as

$$[C_E] = \sum_{i=0}^{\text{rk } \mathfrak{g}} a_i C_{r_i}, \quad (3.27)$$

	$D_{r_1}^X$	$D_{r_2}^X$	$D_{r_3}^X$	$D_{r_4}^X$	$D_{r_5}^X$	$D_{r_6}^X$	D_s^X	D_t^X	D_u^X	D_v^X	D_x^X	D_y^X	D_z^X
C_1	0	1	-2	1	1	0	0	0	0	0	0	0	0
C_2	0	0	1	-2	0	0	1	0	0	0	0	0	0
C_3	0	0	1	0	-2	1	0	0	0	0	0	0	0
C_4	1	-1	0	0	1	-1	0	0	0	0	0	0	0
C_5	-1	1	0	0	0	-1	0	0	0	0	1	0	0
C_6	-1	0	0	0	0	1	0	0	0	0	0	1	0
C_7	0	0	0	1	0	0	-2	0	0	0	0	0	1
C_8	0	0	0	0	0	0	1	1	0	0	0	0	-2
C_9	0	0	0	-1	0	0	-1	0	1	1	0	0	0

Table 3.2: Toric Mori cone generators for an $(E_6)_3$ variety of embedding type I.

with a_i the marks of \mathfrak{g} , i.e. the coefficients of the highest root in an expansion of simple roots.

In this subsection, we will obtain such distinguished curves C_j in the anti-canonical hypersurface X as intersections of two torus invariant divisors of the ambient space Y with the anti-canonical divisor $-K_Y$. Recall that the torus invariant divisors in the homogeneous coordinate ring presentation of a toric variety, which we reviewed briefly in section 3.1, are obtained as zeros of the homogeneous coordinates. To obtain the intersection of these with the anti-canonical divisor, we therefore need to study the zero locus of a generic anti-canonical section, in the presentation (3.7), when the corresponding coordinate, say x_i , is set to zero. We will introduce the notation

$$D_{x_i}^X = -D_{x_i}^Y \cdot K_Y, \quad (3.28)$$

and use the intersection product in the appropriate space as indicated by the superscript of the divisors.

Unlike the case for elliptically fibered surfaces, elliptically fibered threefolds can have singularities associated to non-simply laced Lie algebras. This happens when the fiber of the resolution divisor over a generic point of the discriminant locus is reducible. In such cases, we divide the corresponding curve class obtained as the intersection of two torus invariant divisors by the number n^{comp} of irreducible components, thus obtaining the class of an irreducible component in $N_1(X)$.

The proper identification of the distinguished curves C_j in X turns out to depend on a single condition on the Stanley-Reisner ideal $I_{Stanley-Reisner}$ of the ambient space Y : whether this ideal contains the monomial $u * v$ or not. Given the significance of this condition for the following analysis, we introduced the terminology embedding type I and embedding type II varieties in section 3.5 to distinguish these two cases. We will now discuss them in turn.

3.7.1 Type I: $u * v \in I_{\text{Stanley-Reisner}}$

When $u * v \in I_{\text{Stanley-Reisner}}$, X is fibered over the base \mathbb{F}_n ,

$$\pi : X \rightarrow \mathbb{F}_n, \quad (3.29)$$

with π induced from the projection $N \rightarrow \langle (0, 0, 1, 0), (0, 0, 0, 1) \rangle$ of the lattice carrying the fan of the ambient space of X . $\pi|_Z$ induces a push-forward map (we drop the $|_Z$ in the notation) $\pi_* : N^1(Z) \rightarrow N^1(\mathbb{F}_n)$. We will denote divisor classes both in $N^1(X)$ and $N^1(\mathbb{F}_n)$ by $[\cdot]$. In particular, we write $[D_B^{\mathbb{F}_n}]$ and $[D_F^{\mathbb{F}_n}]$ for the base and fiber class of \mathbb{F}_n .

The divisors that will be relevant in our discussion are the following:

$$D_z^X: \quad [D_z^X] = [Z]$$

$$D_u^X: \quad \pi_*(D_u^X \cdot [Z]) = [D_F^{\mathbb{F}_n}]$$

$$D_s^X: \quad \pi_*([D_s^X] \cdot [Z]) = [D_B^{\mathbb{F}_n}]$$

$$D_{r_i}^X: \quad [D_{r_i}^X] \cdot [Z] = 0$$

By studying the intersection properties of these divisors, we can identify the distinguished curves in the geometry with the following torically invariant intersections:

C_B , the base curve of the Hirzebruch surface

$$C_B = D_z^X \cdot D_s^X \quad (3.30)$$

C_F , the fiber curve of the Hirzebruch surface

$$C_F = D_z^X \cdot D_u^X \quad (3.31)$$

C_{r_0} , the fibral rational curve intersecting the zero section

$$C_{r_0} = D_s^X \cdot D_u^X \quad (3.32)$$

C_{r_i} , the exceptional curves

$$C_{r_i} = \frac{1}{n_i^{\text{comp}}} D_{r_i}^X \cdot D_u^X \quad (3.33)$$

With regard to the discussion in section 2, we identify the $D_{r_i}^X$ with the resolution divisors associated to the perturbative gauge fields A_i ; the curves C_{r_i} , when wrapped by M2 branes, give rise to the vector multiplets associated to the Lie algebra element E_{α_i} , for $\alpha_i \in \Delta$, i.e. a simple root. It follows that the intersection numbers between these divisor and curve classes must reproduce the negative Cartan matrix of a Lie algebra \mathfrak{g} .⁵ In fact, more is true: including $D_{r_0}^X := D_s^X$ and C_{r_0} in our considerations, we have

$$C_{r_i} \cdot D_{r_j}^X = -\widehat{A}_{ij}, \quad i, j = 0, \dots, \text{rk } \mathfrak{g}, \quad (3.35)$$

with \widehat{A} the affine Cartan matrix of \mathfrak{g} .

As the curves C_B and C_F arise via intersections with the divisor D_z^X , the computation of their Mori vectors reduces to a computation of intersection numbers in \mathbb{F}_n . Thus, for C_B , the only non-vanishing intersection numbers are

$$[D_s^X] \cdot [C_B] = [D_s^X] \cdot [D_z^X] \cdot [D_s^X] = [D_B^{\mathbb{F}_n}]^2 = -n, \quad (3.36)$$

$$\begin{aligned} [D_u^X] \cdot [C_B] &= [D_u^X] \cdot [D_z^X] \cdot [D_s^X] = [D_F^{\mathbb{F}_n}] \cdot [D_B^{\mathbb{F}_n}] = 1 \\ &= [D_v^X] \cdot [C_B], \end{aligned} \quad (3.37)$$

$$\begin{aligned} [D_z^X] \cdot [C_B] &= [D_z^X] \cdot [D_z^X] \cdot [D_s^X] = [K^{\mathbb{F}_n}] \cdot [D_B^{\mathbb{F}_n}] \\ &= -(2[D_B^{\mathbb{F}_n}] + (n+2)[D_F^{\mathbb{F}_n}]) \cdot [D_B^{\mathbb{F}_n}] \\ &= 2n - n - 2 = n - 2, \end{aligned} \quad (3.38)$$

while for C_F ,

$$[D_s^X] \cdot [C_F] = [D_s^X] \cdot [D_z^X] \cdot [D_u^X] = [D_B^{\mathbb{F}_n}] \cdot [D_F^{\mathbb{F}_n}] = 1, \quad (3.39)$$

$$\begin{aligned} [D_z^X] \cdot [C_F] &= [D_z^X] \cdot [D_z^X] \cdot [D_u^X] = [K^{\mathbb{F}_n}] \cdot [D_F^{\mathbb{F}_n}] \\ &= -(2[D_B^{\mathbb{F}_n}] + (n+2)[D_F^{\mathbb{F}_n}]) \cdot [D_F^{\mathbb{F}_n}] \\ &= -2. \end{aligned} \quad (3.40)$$

Note that the intersection numbers with the divisors D_v^X and D_t^X follow from the linear equivalences

$$D_v^Y \sim D_u^Y, \quad D_t^Y \sim nD_u^Y + D_s^Y + \sum a_i^\vee D_{r_i}^Y, \quad (3.41)$$

⁵Note that it is the factor $1/n_i^{\text{comp}}$ in relation (3.33) that motivates identifying the divisors $D_{r_i}^X$ with simple coroots and the curves C_{r_i} with simple roots. Indeed, we have

$$\alpha = \frac{1}{n_\alpha} \frac{(\alpha_L, \alpha_L)}{2} \alpha^\vee \quad (3.34)$$

with α_L any of the long simple roots, and $n_\alpha = 1$ for α a long simple root, and $n_\alpha = 2, 3$ for α a short simple root (the 3 occurs for the Lie algebra of G_2).

	$D_{r_1}^X$	$D_{r_2}^X$	$D_{r_3}^X$	$D_{r_4}^X$	$D_{r_5}^X$	$D_{r_6}^X$	D_s^X	D_t^X	D_u^X	D_v^X	D_x^X	D_y^X	D_z^X
C_{r_1}	-2	1	0	0	0	0	0	0	0	0	1	1	0
C_{r_2}	1	-2	1	0	0	0	0	0	0	0	0	1	0
C_{r_3}	0	1	-2	1	1	0	0	0	0	0	0	0	0
C_{r_4}	0	0	1	-2	0	0	1	0	0	0	0	0	0
C_{r_5}	0	0	1	0	-2	1	0	0	0	0	0	0	0
C_{r_6}	0	0	0	0	1	-2	0	0	0	0	1	0	0
C_{r_0}	0	0	0	1	0	0	-2	0	0	0	0	0	1
C_F	0	0	0	0	0	0	1	1	0	0	0	0	-2
C_B	0	0	0	0	0	0	$-n$	0	1	1	0	0	$n-2$

Table 3.3: Intersection numbers for an $(E_6)_n$ variety of embedding type I.

with the coefficients a_i^Y denoting the co-marks of \mathfrak{g} for Y a $(\mathfrak{g})_n$ variety. These relations can be read off the toric data of the resolved ambient geometries, given in appendix A for many $(\mathfrak{g})_n$ varieties. In particular, the class of D_t^Y together with the relation (3.27) allows us to identify the generic elliptic fiber as

C_E , the generic elliptic fiber

$$C_E = D_t^X \cdot D_u^X \quad (3.42)$$

The Mori vector of the generic fiber C_E can also be computed universally: by (3.35),

$$[C_E] \cdot [D_{r_j}] = - \sum_{i=0}^{\text{rk } \mathfrak{g}} a_i(\hat{A})_{ij} = 0. \quad (3.43)$$

Indeed, the only non-vanishing intersections are with D_x , D_y , D_z : the generic fiber is a degree 2, 3 curve respectively in x , y , hence

$$D_x^X \cdot C_E = 3, \quad D_y^X \cdot C_E = 2. \quad (3.44)$$

Finally,

$$D_z^X \cdot C_E = [D_B^{\mathbb{F}_n} + nD_F^{\mathbb{F}_n}] \cdot [D_F^{\mathbb{F}_n}] = 1. \quad (3.45)$$

Example: $(E_6)_n$ Let us consider as an example an $(E_6)_n$ variety. The intersection numbers of the curves C_\bullet just constructed with the divisors $D_{x_i}^X$ are given in table 3.3, for general \mathbb{F}_n . We recognize the negative affine Cartan matrix of E_6 in the upper left block of the table.

	$D_{r_1}^X$	$D_{r_2}^X$	$D_{r_3}^X$	$D_{r_4}^X$	D_s^X	D_t^X	D_u^X	D_v^X	D_x^X	D_y^X	D_z^X
C_{r_1}	-2	1	2	0	0	0	0	0	0	1	0
C_{r_2}	1	-2	0	0	1	0	0	0	0	0	0
C_{r_3}	1	0	-2	1	0	0	0	0	0	0	0
C_{r_4}	0	0	1	-2	0	0	0	0	1	0	0
C_{r_0}	0	1	0	0	-2	0	0	0	0	0	1
C_F	0	0	0	0	1	1	0	0	0	0	-2
C_B	0	0	0	0	-5	0	1	1	0	0	3

Table 3.4: Intersection numbers for an $(F_4)_5$ variety of embedding type I.

Example: $(F_4)_5$ The intersection numbers of the distinguished curves C_\bullet with the divisors $D_{x_i}^X$ are given in table 3.4. We have used $n_3^{comp} = n_4^{comp} = 2$ in the definition of C_{r_3} and C_{r_4} .

3.7.2 Type II: $u * v \notin I_{Stanley-Reisner}$

A number of the geometries we are considering contain a $(-1, -1)$ curve C_{isol} involving the base curve C_B of \mathbb{F}_n . Other than the case $n = 1$, for which this base curve itself is a $(-1, -1)$ curve, C_{isol} takes the form

$$[C_{isol}] = [C_B] - [C_f], \quad C_f \in \{C_{r_0}, C_{r_1}, \dots, C_{r_k}\}. \quad (3.46)$$

Starting with a subdivision for which $u * v \in I_{Stanley-Reisner}$ and flopping C_{isol} yields a birationally equivalent hypersurface \tilde{X} with exceptional curve $\tilde{C}_{isol} = D_u^X \cdot D_v^X$.⁶ In particular, this flop leads to cones in the fan which contain both u_{ρ_u} and u_{ρ_v} . Upon such flops, the fibration structure over the base \mathbb{F}_n we began with is lost: in terms of homogeneous coordinates, the variables u and v are now permitted to simultaneously vanish, i.e. $u * v \notin I_{Stanley-Reisner}$, hence no longer parametrize the base \mathbb{P}^1 of \mathbb{F}_n .

We can obtain the distinguished curve classes for a geometry with $u * v \notin I_{Stanley-Reisner}$ by following the torus invariant curves identified in subsection 3.7.1 through the flop. The divisors that do not intersect C_{isol} are not disturbed by the flop. Let $\{D_i^X\}_{i \in I}$ be the set of divisors of \tilde{X} with positive intersection with \tilde{C}_{isol} . Curves in X of the form $D_i^X \cdot D_u^X$ or $D_i^X \cdot D_j^X$ for $i, j \in I$ then have the same Mori vectors as the curves $D_i^X \cdot D_u^X + \tilde{C}_{isol}$, $D_i^X \cdot D_j^X + \tilde{C}_{isol}$ respectively in \tilde{X} .

⁶By comparing images in the singular variety $X \rightarrow \tilde{X} \leftarrow X'$, we can speak of the same set of divisors on X and X'

	$D_{r_1}^X$	$D_{r_2}^X$	$D_{r_3}^X$	$D_{r_4}^X$	$D_{r_5}^X$	$D_{r_6}^X$	$D_{r_7}^X$	D_s^X	D_t^X	D_u^X	D_v^X	D_x^X	D_y^X	D_z^X
C_{r_1}	-2	0	0	0	1	0	1	0	0	0	0	1	0	0
C_{r_2}	0	-2	1	0	1	1	0	0	0	0	0	0	0	0
C_{r_3}	0	1	-2	1	0	0	0	0	0	0	0	0	0	0
C_{r_4}	0	0	1	-3	0	0	0	0	0	1	1	0	0	0
C_{r_5}	1	1	0	0	-2	0	0	0	0	0	0	0	0	0
C_{r_6}	0	1	0	0	0	-2	0	0	0	0	0	0	1	0
C_{r_7}	1	0	0	0	0	0	-2	0	0	0	0	0	1	0
C_{r_0}	0	0	0	0	0	0	0	-3	0	1	1	0	0	1
C_F	0	0	0	0	0	0	0	1	1	0	0	0	0	-2
C_B	0	0	0	0	0	0	0	-3	0	1	1	0	0	1

Table 3.5: Intersection numbers for $(E_7)_3$ varieties of embedding type II.

Example: $(E_7)_3$ The intersection numbers of the distinguished curves C_\bullet introduced in subsection 3.7.1 with the divisors $D_{x_i}^X$ are recorded in table 3.5. Note that the upper left hand corner of this table does not quite reproduce the negative Cartan matrix of E_7 . The Mori vector of the isolated curve $\tilde{C}_{isol} = D_u^X \cdot D_v^X$ is

	$D_{r_1}^X$	$D_{r_2}^X$	$D_{r_3}^X$	$D_{r_4}^X$	$D_{r_5}^X$	$D_{r_6}^X$	$D_{r_7}^X$	D_s^X	D_t^X	D_u^X	D_v^X	D_x^X	D_y^X	D_z^X
\tilde{C}_{isol}	0	0	0	1	0	0	0	1	0	-1	-1	0	0	0

Replacing C_{r_4} and C_s in table 3.5 by $C_{r_4} + \tilde{C}_{isol}$, $C_s + \tilde{C}_{isol}$ reproduces the intersection matrix of an E_7 fibration over \mathbb{F}_3 . Note also that $[D_{r_4}^X \cdot D_s^X] + [\tilde{C}_{isol}] = 0$, allowing us to identify $C_{isol} = D_{r_4}^X \cdot D_s^X$.

Example: $(A_2)_3$ Among all the geometries we consider, this is the only one for which all maximal projective subdivisions of the lattice polytope P_{sing} have $u * v \in I_{Stanley-Reisner}$, i.e. $(A_2)_3$ does not have an element of embedding type I. The intersection numbers of the distinguished curves C_\bullet introduced in subsection 3.7.1 with the divisors $D_{x_i}^X$ are recorded in table 3.6.

The Mori vector of the exceptional curve \tilde{C}_{isol} is

	$D_{r_1}^X$	$D_{r_2}^X$	D_s^X	D_t^X	D_u^X	D_v^X	D_x^X	D_y^X	D_z^X
\tilde{C}_{isol}	1	1	1	0	-1	-1	0	0	0

Replacing C_\bullet for $\bullet \in \{r_1, r_2, E\}$ by $C_\bullet + \tilde{C}_{isol}$, we obtain an intersection matrix with the negative Cartan matrix of affine A_2 appearing in the upper left corner.

	$D_{r_1}^X$	$D_{r_2}^X$	D_s^X	D_t^X	D_u^X	D_v^X	D_x^X	D_y^X	D_z^X
C_{r_1}	-3	0	0	0	1	1	1	3	0
C_{r_2}	0	-3	0	0	1	1	1	0	0
C_{r_0}	0	0	-3	0	1	1	0	0	1
C_F	0	0	1	1	0	0	0	0	-2
C_B	0	0	-3	0	1	1	0	0	1

Table 3.6: Intersection numbers for the $(A_2)_3$ variety. .

3.8 Constructing Higgsing trees torically

Using the formalism developed in this section, we can set up a simple algorithm to determine which singularities can occur torically over a given Hirzebruch base \mathbb{F}_n . Special attention must be paid to cases in which the occurring singularity depends not only on the power of s in the individual coefficients in the Tate form of the elliptic fibration, but also on factorization conditions involving relations between multiple coefficients. The authors of [4] retain the Kodaira name of the (surface) singularity in these cases, but add a superscript ns, s for when factoring does not occur (the ‘non-split’ case, with lower rank singularity), and when it does (the ‘split’ case, with higher rank singularity); in the sole case of the I_0^* singularity, the polynomial in question is of order 3, and also an intermediate factoring condition, indexed by ss (for semi-split), is necessary. When factorization is possible, a variable redefinition can lead to higher order vanishing of appropriate coefficients of the generic section, and thus to a higher rank singularity.

The first step in the algorithm is to construct the polytope P_{sing} as introduced in subsection 3.3. If $P_{sing} \cap M \neq S_{sing}$, the singularity cannot be constructed torically over the given base. If $P_{sing} \cap M = S_{sing}$ but $h^{1,1}(X) - 3$ does not equal the rank of any of the Lie algebras associated to the singularity, the geometry is not suitable for an F-theory compactification [13]. This criterion excludes in particular $n = 9, 10, 11$ completely. Otherwise, the question of factorization can be settled by computing $h^{1,1}(X)$, which reveals the rank of the Lie algebra associated to the singularity. The conclusion can then be checked by computing the intersection matrix between distinguished divisors and curves, as outlined in subsection 3.7. If the correction term

$$\sum_{\Theta^\circ \in F_2(P^\circ)} l^*(\Theta^\circ) l^*(\Theta) \quad (3.47)$$

to $h^{1,1}(X)$ vanishes, the intersections of the toric divisors of Y with X are irreducible, and the generators of the Picard group of X are in 1-1 correspondence with those of Y . In this case, the upper left corner of the intersection matrix as presented e.g. in table 3.3 directly yields the negative Cartan matrix of the associated Lie algebra. When the correction term is non-vanishing, the matrix computed following the steps outlined in section 3.7 can be obtained from the negative Cartan matrix of the Lie algebra associated to the singularity

by summing rows and columns corresponding to the irreducible components of the reducible intersections.

When the correction term is non-vanishing, one can be tempted to modify the geometry to obtain a better toric embedding of X . As we see from (3.47), the only toric divisors of Y which may have reducible intersections with X are those that correspond to cone generators which lie in codimension 2 faces Θ° of P° . The intersection of such divisors with X are reducible if the corresponding dual face Θ , a 1-face of P , contains interior points. Chipping away at these 1-faces by removing an endpoint of the 1-face from S_{sing} ⁷ often leads to an admissible geometry with reduced correction term (3.47). However, the geometry thus obtained may no longer coincide with X .

Example: $(G_2)_4$ Following the above procedure naively suggests that a G_2 singularity can be imposed over \mathbb{F}_4 , but the resulting resolved hypersurface X has $h^{1,1}(X) = 7$. This indicates that in fact, the imposed singularity must have rank 4, suggesting its identification as D_4 (i.e. $I_0^{*ns} \rightarrow I_0^{*s}$). We can check this conclusion by computing the intersection matrix of the distinguished curves C_\bullet of the geometry with the toric invariant divisors, which we give in table 3.7. The analysis is complicated by the fact that for this example, some divisors

	$D_{r_1}^X$	$D_{r_2}^X$	D_s^X	D_t^X	D_u^X	D_v^X	D_x^X	D_y^X	D_z^X
C_{r_1}	-2	1	0	0	0	0	0	1	0
C_{r_2}	3	-2	1	0	0	0	1	0	0
C_{r_0}	0	1	-2	0	0	0	0	0	1
C_F	0	0	1	1	0	0	0	0	-2
C_B	0	0	-4	0	1	1	0	0	2

Table 3.7: Intersection numbers for a $(G_2)_4$ variety. .

of the ambient space Y intersect the hypersurface X reducibly; the value of the correction term (3.47) is 2. In particular, the negative Cartan matrix appearing in the upper left corner of the table is that of G_2 . By decomposing $D_{r_1}^X$ in terms of irreducible components

$$D_{r_1}^X = D_{r_{1,1}}^X + D_{r_{1,2}}^X + D_{r_{1,3}}^X, \quad (3.48)$$

⁷Generically, only one choice leads to a compact P_{sing} .

we can see that the intersection numbers given in table 3.7 are indeed consistent with the hypersurface X resulting from the resolution of a D_4 singularity:

$$C_{D_4} = \begin{pmatrix} 2 & -1 & 0 & 0 \\ -1 & 2 & -1 & -1 \\ 0 & -1 & 2 & 0 \\ 0 & -1 & 0 & 2 \end{pmatrix} \rightarrow \begin{pmatrix} 2 & -3 & 2 & 2 \\ -1 & 2 & -1 & -1 \end{pmatrix} \rightarrow \begin{pmatrix} 6 & -3 \\ -3 & 2 \end{pmatrix} \rightarrow \begin{pmatrix} 2 & -1 \\ -3 & 2 \end{pmatrix} = C_{G_2} \quad (3.49)$$

We can try to reduce the value 2 of the correction term (3.47) by applying the excision procedure outlined above twice. The first application does not modify X while reducing the correction term by 1. One can obtain the same toric data by directly imposing a D_4 singularity over \mathbb{F}_4 to obtain P_{sing} . A second application however changes the geometry to a B_4 singularity over \mathbb{F}_4 .⁸

Following the procedure outlined in this subsection, we reproduce all gauge groups occurring in the Higgsing trees over \mathbb{F}_n [4, 20] with vanishing correction term (3.47) except for

- The symplectic groups over \mathbb{F}_2 : attempting to impose the I_{2k}^{ns} singularities automatically leads to I_{2k}^s singularities,
- Over \mathbb{F}_1 and \mathbb{F}_2 , both B_5 and D_6 singularities can be imposed, but only B_5 can be imposed torically.
- Over \mathbb{F}_4 , a D_4 singularity can be imposed, but one divisor of the ambient space intersects the hypersurface reducibly.

4 Computing genus 0 Gromov-Witten invariants via mirror symmetry

Mirror symmetry maps the problem of computing the genus 0 Gromov-Witten invariants n_k of a Calabi-Yau manifold X to that of computing the appropriate periods of the top form $[\Omega] \in H^{(3,0)}(X')$ of the holomorphic Dolbeault cohomology ring on the mirror Calabi-Yau manifold X' .

The generating function for the genus 0 Gromov-Witten invariants of X is called the prepotential $F(\mathbf{t})$. It is computed [47, 48] by the topological string A-model on X ; the variable dependence (\mathbf{t}) is on flat coordinates \mathbf{t} on the Kähler structure moduli space $\mathcal{M}_J(X)$ of X .

⁸This contradicts a statement in [16, 24]. It appears however that the genus 0 Gromov-Witten invariants of $(D4)_4$ and $(B4)_4$, in as far as these enter into the considerations of these two references, coincide. We are currently investigating this phenomenon.

It takes the universal form

$$F(\mathbf{t}) = \frac{c_3(X)}{(2\pi i)^3} \zeta(3) + \sum_i \frac{c_2(X) \cdot D_i}{24} t_i + \frac{1}{3!} \sum_{i,j,k} d_{ijk} t_i t_j t_k + \sum_{\mathbf{k}, n} \frac{n_{\mathbf{k}}}{n^3} e^{2\pi i n \mathbf{k} \cdot \mathbf{t}}, \quad (4.1)$$

where D_i are divisor classes associated to the coordinate t_i , and $d_{ijk} = D_i \cdot D_j \cdot D_k$. The coefficients of the polynomial (perturbative) terms in \mathbf{t} depend on topological invariants of X , whereas the coefficients of the exponential (non-perturbative) terms are the enumerative invariants that we are after.

Mirror symmetry is the statement that the prepotential $F(\mathbf{t})$ on X can be entirely computed from period computations on the mirror manifold X' . The periods in question are those of an appropriately normalized representative Ω of $H^{(3,0)}(X')$. To express $F(\mathbf{t})$ in terms of these, one must choose a symplectic basis $\{\alpha_I, \beta_I\}$ of $H_3(X', \mathbb{Z})$ (discussed below in subsection 4.1.5), and write

$$X_I = \int_{\alpha_I} \Omega, \quad F_I = \int_{\beta_I} \Omega. \quad (4.2)$$

We will refer to the X_I as the A -periods of Ω , and the F_I as the B -periods. A theorem of Bryant and Griffiths [49] implies that when the basis of cycle classes is chosen appropriately, the B -periods F_I are fully determined in terms of the A -periods X_I . As Ω is determined by its periods, we can write $\Omega(\mathbf{X})$. With regard to the complex structure determined by the periods \mathbf{X}^0 (i.e. such that $[\Omega(\mathbf{X}^0)] \in H^{(3,0)}(X')$), a local argument implies

$$[\partial_{X_I} \Big|_{\mathbf{X}=\mathbf{X}^0} \Omega(\mathbf{X})] \in H^{(3,0)}(X') \oplus H^{(2,1)}(X'). \quad (4.3)$$

Hence,

$$0 = \int \Omega(\mathbf{X}^0) \wedge \partial_{X_I} \Big|_{\mathbf{X}=\mathbf{X}^0} \Omega(\mathbf{X}). \quad (4.4)$$

By the Riemann bilinear identities,

$$0 = \sum_J X_J^0 \partial_{X_I} \Big|_{\mathbf{X}=\mathbf{X}^0} F_J(\mathbf{X}) - F_I(\mathbf{X}^0), \quad (4.5)$$

whence

$$2F_I(\mathbf{X}^0) = \partial_{X_I} \Big|_{\mathbf{X}=\mathbf{X}^0} \sum_J X_J F_J(\mathbf{X}). \quad (4.6)$$

It follows that the period $F_I(\mathbf{X})$ can be obtained as the X_I derivative

$$F_I(\mathbf{X}) = \partial_{X_I} F(\mathbf{X}) \quad (4.7)$$

of one quantity $F(\mathbf{X})$, defined as

$$F(\mathbf{X}) = \frac{1}{2} \sum_J X_J F_J(\mathbf{X}). \quad (4.8)$$

This is the definition of the prepotential based on complex structure data of X' . The statement of mirror symmetry is that upon an appropriate choice of basis of $H_3(X', \mathbb{Z})$ discussed below, the variable identification

$$t_i = \frac{X_i}{X_0} \quad (4.9)$$

allows us to equate

$$F(\mathbf{X}) = X_0^2 F\left(1, \frac{X_i}{X_0}\right) = X_0^2 F(\mathbf{t}). \quad (4.10)$$

$F(\mathbf{t})$ here denotes the A -model prepotential (4.1), $F(\mathbf{X})$ the period expression (4.8), whose homogeneity of degree 2 property (which follows from its definition) we have used.

In the following subsection, we will fill in the details required to explicitly perform the computation of $F(\mathbf{X})$ in the class of anti-canonical hypersurfaces of toric varieties. In a nutshell, the steps required are the following:

1. Write down a representative for the class of Ω as a function of appropriate coordinates on $\mathcal{M}_{\text{cplx}}(X')$.
2. Find a complete system of differential equations (the Picard-Fuchs system) satisfied by these periods. While it is possible to compute periods by identifying cycles in $H_3(X', \mathbb{Z})$ and performing integrals, it is much more convenient to compute them as solutions of the Picard-Fuchs system.
3. Identify the linear combination of solutions corresponding to the appropriate symplectic basis of $H_3(X')$. The fastest route to this identification is by imposing the perturbative part of $F(\mathbf{t})$ given in terms of the topological invariants of X as written in (4.1). Note that having recourse to (easily computable) data of X is for computational convenience only.

4.1 Mirror symmetry for hypersurfaces in toric varieties: an algorithm for computing their Gromov-Witten invariants

The theory of mirror symmetry on Calabi-Yau hypersurfaces of toric varieties is very well developed [28, 40].⁹ In this subsection, we will review all aspects required to understand

⁹The theory of complete intersections is similar in many aspects [41, 50], but we will not be discussing it here.

the algorithm for the computation of the genus 0 Gromov-Witten invariants for this class of Calabi-Yau threefolds. Aside from the original references, most of the material reviewed here can be found in the book [42].

A point on notation: The mirror family to the anti-canonical hypersurface X sitting inside the toric variety Y_Σ , where Σ is a maximal projective subdivision of a lattice polytope P , is given by anti-canonical hypersurfaces X' sitting inside the toric variety $Y'_{\Sigma'}$, where Σ' is a maximal projective subdivision of a lattice polytope P° , the polar polytope to P . It is standard to designate the lattice of one-parameter subgroups of the torus $T_N \subset Y$ by the letter N , and its character lattice by the letter M . For the mirror hypersurface, we have $T_M \subset Y'$, and M and N are exchanged. We feel that this exchange on casual reading can be a source of confusion. We hope to alleviate this by introducing the notation $M^\circ = M^\vee = N$, $N^\circ = N^\vee = M$.

4.1.1 A representative of Ω in appropriate coordinates on the complex structure moduli space $\mathcal{M}_{cplx}(X')$

When X' is an anti-canonical hypersurface of a toric variety Y' , we can obtain a representative Ω of a generator of $H^{3,0}(X')$ as the residue of the extension of the form

$$\omega = \frac{1}{f} \frac{dt_1}{t_1} \wedge \dots \wedge \frac{dt_4}{t_4}, \quad (4.11)$$

defined on the torus $T \subset Y'$ [51]. Here, t_i are natural coordinates on $T \cong (\mathbb{C}^*)^4$ (not to be confused by coordinates on the moduli space $\mathcal{M}_J(X)$), and in the notation introduced in (3.5), $f \in L(P^\circ)$. f yields the hypersurface X' as its zero locus, $f = 0$. It has the form

$$f = \sum_i \lambda_i \mathbf{t}^{m_i}, \quad \mathbf{t}^{m_i} = \prod_j t_j^{(m_i)_j}, \quad (4.12)$$

with the sum over the index set parametrizing the $r + 1$ points $m_i \in P^\circ \cap M^\circ$. For later convenience, we will assign the origin the index 0, $m_0 = \mathbf{0}$.

Before computing the periods of Ω , we need to express ω in terms of good coordinates on the complex structure moduli space $\mathcal{M}_{cplx}(X')$. The coefficients $\{\lambda_i\}$ occurring in (4.12) parametrize $\mathcal{M}_{cplx}(X')$ redundantly:

- T acts on itself and thus on f , leading to isomorphic hypersurfaces, via

$$\boldsymbol{\nu} \cdot f = \sum_i \lambda_i (\boldsymbol{\nu} \cdot \mathbf{t})^{m_i}, \quad \boldsymbol{\nu} \in T. \quad (4.13)$$

- Rescaling of f by a non-zero constant $c \in \mathbb{C}^*$ does not change its zero locus.

To eliminate this $T \times \mathbb{C}^*$ redundancy, we can consider a basis of the lattice Λ of relations amongst the r vectors m_i , $i \neq 0$. As we are considering four dimensional ambient spaces, upon a choice of generating set for M° , $m_i \in \mathbb{Z}^4$; there will hence be $r - 4$ such relations. We will label these as l^α , $\alpha = 1, \dots, r - 4$, such that

$$\sum_{i=1}^r (l^\alpha)_i m_i = 0, \quad \alpha = 1, \dots, r - 4. \quad (4.14)$$

The coordinates

$$z_\alpha = \lambda_0^{-\sum_{i=1}^r (l^\alpha)_i} \prod_{i=1}^r \lambda_i^{(l^\alpha)_i} \quad (4.15)$$

are then invariant under the $T \times \mathbb{C}^*$ action. Note that upon introducing the set of points

$$\Xi = 1 \times (P^\circ \cap M^\circ) \quad (4.16)$$

in \mathbb{Z}^5 , the basis of relations l^α of points $P^\circ \cap M^\circ$ is naturally extended to a basis of relations L^α of the points Ξ , in terms of which the coordinates z_α are expressed as

$$z_\alpha = \prod_{i=0}^r \lambda_i^{(L^\alpha)_i}. \quad (4.17)$$

Either way, the z_α coordinatize the quotient

$$L(P^\circ)/T \times \mathbb{C}^* = \mathbb{P}(L(P^\circ))/T, \quad (4.18)$$

which is a first approximation to the complex structure moduli space $\mathcal{M}_{cplx}(X')$.

The choice of coordinates on the space (4.18) thus maps to a choice of basis $\{L^\alpha\}$ on the space of relations among the points of Ξ . We will discuss this choice further in sections 4.1.4 and 4.2.

4.1.2 The Picard-Fuchs system

Rather than calculating the periods of Ω directly by identifying appropriate cycles in X' and integrating, it is computationally more convenient to derive a set of differential operators which annihilate these periods. The complete set of such operators (i.e. such that each element of their joint kernel is a linear combination of periods) spans the so-called Picard-Fuchs ideal. The problem of computing periods is thus mapped to finding the general family of solutions of a set of differential equations, and identifying the linear combinations of solutions corresponding to periods with regard to an appropriate basis of $H_3(X', \mathbb{Z})$.

Given the explicit expression (4.11) for ω , it is not difficult to derive elements of the Picard-Fuchs ideal. To this end, for any relation L among the points Ξ , we define the differential

operator \square_L via

$$\square_L = \prod_{L_i > 0} \theta_i^{L_i} - \prod_{L_i < 0} \theta_i^{-L_i}, \quad (4.19)$$

with θ_i the logarithmic derivative

$$\theta_i = \frac{1}{\lambda_i} \frac{\partial}{\partial \lambda_i}. \quad (4.20)$$

It is then a simple calculation to check that

$$\square_L \omega = 0. \quad (4.21)$$

Multiplying ω by λ_0 to render it invariant under the \mathbb{C}^* action, we obtain a set of Picard-Fuchs operators

$$\square_{L^\alpha} \frac{1}{\lambda_0}, \quad \alpha = 1, \dots, r-4. \quad (4.22)$$

This set however generically does not generate the complete Picard-Fuchs ideal. Methods for obtaining the missing differential operators in the case of toric hypersurfaces are discussed in [28].

4.1.3 A distinguished basis of periods at a MUM point

Determining the Gromov-Witten invariants of X requires computing the periods of Ω at a point in $\mathcal{M}_{cplx}(X')$ that is mirror to the large radius point of X . Matching the expected structure of the periods suggests that this should be a point of maximally unipotent monodromy (a MUM point) [52]: at such a point, all indices are equal (and in fact vanish). Introducing local coordinates z_i on $\mathcal{M}_{cplx}(X')$ such that a boundary point p of $\mathcal{M}_{cplx}(X')$, $p \in \overline{\mathcal{M}}_{cplx}(X') - \mathcal{M}_{cplx}(X')$, is given by the vanishing of these coordinates, p is a MUM point if exactly one period is analytic here, and $h^{1,1}(X)$ periods have logarithmic growth in z_i . One can include as part of the definition of the MUM point that integer linear combinations of the logarithmic periods exist which each have logarithmic growth with regard to exactly one coordinate z_i .

In the toric case, a basis of periods at a MUM point can be computed as follows. Power series solutions to the Picard-Fuchs system around the point $\mathbf{z} = \mathbf{0}$ are given by¹⁰

$$\Pi_{power}(\mathbf{z}; \boldsymbol{\rho}) = \sum_{\mathbf{n} \in \mathbb{N}_0^{h^{1,1}(X)}} \frac{\Gamma(1 - \sum_{\alpha} (n_{\alpha} + \rho_{\alpha})(L^{\alpha})_0)}{\prod_{i>0} \Gamma(1 + \sum_{\alpha} (n_{\alpha} + \rho_{\alpha})(L^{\alpha})_i)} \frac{\prod_{i>0} \Gamma(1 + \sum_{\alpha} \rho_{\alpha}(L^{\alpha})_i)}{\Gamma(1 - \sum_{\alpha} \rho_{\alpha}(L^{\alpha})_0)} \mathbf{z}^{\mathbf{n} + \boldsymbol{\rho}}, \quad (4.23)$$

where $\boldsymbol{\rho}$ is any of the $2 + 2h^{1,1}(X)$ (not necessarily distinct) indices of the system. At a point at which all indices vanish, there exists a unique holomorphic solution Π_0 , obtained by setting $\boldsymbol{\rho} = \mathbf{0}$ in (4.23). Π_0 can then be completed to a basis of solutions via the Frobenius

¹⁰To be precise, the coordinates \mathbf{z} used here differ from those introduced in (4.17) by signs $(-1)^{(L^{\alpha})_0}$.

method:

$$\Pi_0 = \Pi_{power}(\mathbf{z}; 0), \quad (4.24)$$

$$\Pi_\alpha = \partial_{\rho_\alpha} \Big|_{\boldsymbol{\rho}=\mathbf{0}} \Pi_{power}(\mathbf{z}; \boldsymbol{\rho}), \quad (4.25)$$

$$\Pi_{\alpha,\beta} = \partial_{\rho_\alpha} \partial_{\rho_\beta} \Big|_{\boldsymbol{\rho}=\mathbf{0}} \Pi_{power}(\mathbf{z}; \boldsymbol{\rho}), \quad (4.26)$$

$$\Pi_{\alpha,\beta,\gamma} = \partial_{\rho_\alpha} \partial_{\rho_\beta} \partial_{\rho_\gamma} \Big|_{\boldsymbol{\rho}=\mathbf{0}} \Pi_{power}(\mathbf{z}; \boldsymbol{\rho}). \quad (4.27)$$

A complete set of solutions of the Picard-Fuchs system at such a point therefore consists of one holomorphic, $h^{1,1}(X)$ logarithmic, $h^{1,1}(X)$ doubly logarithmic, and one triply logarithmic solution.

Extracting Gromov-Witten invariants from the Picard-Fuchs system requires identifying appropriate linear combinations of these solutions, corresponding to the choice of an appropriate symplectic basis of $H_3(X', \mathbb{Z})$. To address this task, we need to take a closer look at the choice of variables \mathbf{z} on $\mathcal{M}_{cplx}(X')$.

4.1.4 How to choose coordinates on complex structure moduli space – the prequel

The choice of variables z_α , and thus the point in complex structure moduli space that $\mathbf{z} = \mathbf{0}$ designates, clearly depends on the choice of basis $\{l_\alpha\}$ for the lattice of relations Λ of the points $P^\circ \cap M^\circ$ introduced in (4.14). Note that as P° is reflexive, its only interior point is the origin. All other elements of the intersection are thus vertices of P° , hence elements of $\Sigma(1)$. Now recall from subsection 3.6 that on X , every curve C gives rise to a relation amongst the elements of $\Sigma(1)$, as encoded in the Mori vector of the curve. The generators of the Mori cone yield a basis of all such relations. We have thus identified generators of Λ whose duals generate the Kähler cone of X . As mirror symmetry between X and X' requires relating $\mathcal{M}_J(X)$ to $\mathcal{M}_{cplx}(X')$, it is a natural conjecture [53] that the sought after basis of Λ determining distinguished coordinates \mathbf{z} on $\mathcal{M}_{cplx}(X')$ should be given by these generators.

In practice, as discussed in subsection 3.6, we generally do not have a basis of the Mori cone of X at our disposal. We will discuss the repercussions of this fact in the context of the class of examples we are considering in section 4.2, after we have completed our discussion of how to compute the prepotential on anti-canonical hypersurfaces of toric varieties, assuming an appropriate choice of basis of Λ has been found.

4.1.5 Identifying the linear combinations of solutions which coincide with periods of Ω in a symplectic basis of $H_3(X', \mathbb{Z})$

We can identify the periods Π_0 and Π_α introduced in (4.23) and (4.24) with the A -periods X_0 and X_i of Ω . By invoking mirror symmetry, this can be argued for by studying the leading behavior of contributions to the mirror volume form $\int \Omega \wedge \bar{\Omega}$ in the variables t_i . Having identified X_0 and X_i allows us to compute the coordinates t_i via (4.9). Linear combinations of the periods $\Pi_{\alpha,\beta}$ must then describe the B -periods F_i dual to the logarithmic periods X_i , $i = 1, \dots, h^{1,1}(X)$. To find the appropriate linear combinations, we invoke mirror symmetry, which identifies the symplectic product of periods (4.8) with the prepotential (4.1), upon imposition of the mirror map (4.9). Given (4.7), the perturbative contribution to $F(\mathbf{t})$ which is cubic in t_i supplies sufficient information to fix the periods F_i in terms of $\Pi_{\alpha,\beta}$. These in turn can be integrated to obtain the non-perturbative piece of $F(\mathbf{t})$, the generating function for Gromov-Witten invariants.

4.2 How to choose coordinates on complex structure moduli space

As discussed in section 3.6, any projective subdivision of the lattice polytope P gives rise to a fan Σ and a projective variety Y_Σ with associated Kähler cone $\text{Nef}(Y_\Sigma)$ and the associated dual cone, the Mori cone $\overline{\text{NE}}(Y_\Sigma)$ of Y_Σ . The corresponding cones of the hypersurface X sitting inside Y_Σ are generically larger, $\text{Nef}(Y_\Sigma) \subset \text{Nef}(X)$ and smaller $\overline{\text{NE}}(X) \subset \overline{\text{NE}}(Y_\Sigma)$, respectively. We have found experimentally that the Gromov-Witten invariants of X can be calculated using any smooth cone $\mathcal{C}(X) \subset \text{Nef}(X)$, as long as for each generator of $\mathcal{C}(X)$, the sum of its entries is non-negative, i.e. a putative associated curve does not violate the nef condition on the anti-canonical class of X .

The most naive choice for $\mathcal{C}(X)$ is $\text{Nef}(Y_\Sigma)$ for any projective subdivision Σ of P such that $X \subset Y_\Sigma$. The following situations may occur:

1. If $\text{Nef}(Y_\Sigma)$ is smooth, the algorithm outlined in section 4.1 based on $\text{Nef}(Y_\Sigma)$ will yield the Gromov-Witten invariants of X . Depending on how well $\text{Nef}(Y_\Sigma)$ approximates $\text{Nef}(X)$, many of the invariants computed in the basis provided by the generators of $\text{Nef}(Y_\Sigma)$ will vanish.
2. $\text{Nef}(Y_\Sigma)$ is not smooth, but it is top dimensional (i.e. has the dimension of $N^1(X)$) and simplicial. Appropriately refining $\text{Nef}(Y_\Sigma)$ leads to smooth subcones contained in $\text{Nef}(X)$. Any such subcone leads to the correct Gromov-Witten invariants of X , provided that for each generator of the subcone, the sum of its entries is non-negative.
3. $\text{Nef}(Y_\Sigma)$ is top dimensional but not simplicial. In this case, we can consider simplicial subdivisions of $\text{Nef}(Y_\Sigma)$ as a starting point for 2.
4. $\text{Nef}(Y_\Sigma)$ is not top dimensional. This occurs when $\overline{\text{NE}}(X)$ is not strictly convex, i.e.

when pairs of curves exist whose Mori vectors map to each other upon multiplication by -1 . Such subdivisions Σ do not provide a convenient approximation to $\text{Nef}(X)$ for the computation of the Gromov-Witten invariants of X .

A better approximation to $\text{Nef}(X)$ than $\text{Nef}(Y_\Sigma)$ for $X \subset Y_\Sigma$ is the dual of the toric Mori cone (3.26) which we introduced in section 3.6. In most geometries that we have studied, this cone is smooth. When it is not, the steps outlined above must be pursued to obtain from it a cone on which the mirror symmetry algorithm can be based.

4.3 The Gromov-Witten invariants of interest

The interpretation of Gromov-Witten invariants is simplest when all of the curves in a given class are isolated. In this case, the invariant yields the number of such curves. Another simple case [54] is when the curves in a given class are parametrized by a smooth variety B of dimension b . Then the invariant is given by $c_b(\Omega_B^1)$, the appropriate Chern number of the holomorphic cotangent bundle of B . These are the two cases that occur in our considerations together with a third hybrid case: the moduli space of the curves in a given class is disconnected, containing both a family and isolated curves. In this case, the invariant is the sum of the invariants of all components.

4.4 Gromov-Witten invariants of birationally equivalent varieties

Following early results assuming genericity [55,56], the flop invariance of the genus 0 topological string partition function was proved in [57].¹¹ At the level of Gromov-Witten invariants, this implies that curves lying in the intersection of the Mori cones (identified via their image to the common singular manifold with the exceptional locus removed) of two varieties related by a flop have the same Gromov-Witten invariants. We can easily check this for all of our examples.

5 Identifying matter: the formalism applied

We are at long last ready to apply the formalism developed above to determine the gauge algebra \mathfrak{g} and the matter content $\bigoplus_i \mathfrak{R}_i$, with \mathfrak{R}_i denoting representations of \mathfrak{g} , of an F-theory compactification on the elliptically fibered anti-canonical hypersurface X .

¹¹Note that [55] shows a stronger result for a particular example: that the genus 0 topological string free energy coincides for the two birationally equivalent manifolds upon analytic continuation in the Kähler parameter of the flopped curve. Here, we are merely considering the Gromov-Witten invariants outside the locus in which the two varieties differ.

5.1 Embedding the root lattice $\Lambda^{root}(\mathfrak{g})$ in $N_1(X)$

Using our results from section 3.7, we can identify the distinguished curves in X within the toric Mori cone (or, when the latter is not smooth, within the dual of the smooth refinement of the toric Kähler cone) with regard to which we compute the Gromov-Witten invariants of X . In the notation of 3.7, our analysis will be based on curves with no component in the classes of C_B , C_F , and C_{r_0} .

As discussed in section 2, curves which give rise to fields residing in vector multiplets come in \mathbb{P}^1 families. These are hence identifiable via the Gromov-Witten invariants $c_1(\Omega_{\mathbb{P}^1}^1) = -2$. The curves in X with vanishing $[C_B]$, $[C_F]$, and $[C_{r_0}]$ components and Gromov-Witten invariant -2 will furnish a basis of the root lattice of \mathfrak{g} (up to a subtlety we shall discuss in section 5.2.2). Comparing the intersection matrix of these curves with the divisors $D_{r_i}^X$ to Dynkin diagrams of simple Lie algebras allows us to identify \mathfrak{g} , and to define a linear embedding ϕ of the root lattice $\Lambda^{root}(\mathfrak{g})$ of \mathfrak{g} into $N_1(X)$, with image inside the Mori cone of X :

$$\phi : \Lambda^{root}(\mathfrak{g}) \rightarrow N_1(X). \quad (5.1)$$

5.2 Identifying matter

All remaining curves with vanishing $[C_B]$, $[C_F]$, and $[C_{r_0}]$ components are isolated, hence give rise to fields residing in charged matter hypermultiplets. By section 4.3, the Gromov-Witten invariants associated to the class of such curves count their number (unless non-isolated curves lie in the same class; this is the hybrid case invoked in section 4.3 and discussed further in section 5.2.2). The Mori vectors of such curves lie in the image of ϕ extended over \mathbb{Q} . Their inverse image under $\phi_{\mathbb{Q}}$ lies inside the weight lattice $\Lambda^{weight}(\mathfrak{g})$ of \mathfrak{g} .

Recall that $\Lambda^{weight} = (\Lambda^{root})_{\mathbb{Q}}$, i.e. weights λ expanded in a basis of simple roots will exhibit rational coefficients. Nevertheless, the image under $\phi_{\mathbb{Q}}$ of those weights that belong to representations \mathfrak{R}_i furnished by X lies in $N_1(X)$.

5.2.1 Complex vs. self-conjugate representations

Given the Gromov-Witten invariant associated to a curve class giving rise to fields residing in a hypermultiplet transforming in the representation \mathfrak{R} , determining the number of such hypermultiplets depends on whether the representation \mathfrak{R} is complex or (pseudo-)real.

Let $S(\mathfrak{R})$ be the set of curves that give rise to the scalars in the representation \mathfrak{R} . The collection $S(\mathfrak{R})$ will generically contain both holomorphic and anti-holomorphic curves. Only the holomorphic elements are counted by Gromov-Witten invariants.

If the representation \mathfrak{R} is complex, then $\lambda \in \Pi(\mathfrak{R}) \rightarrow -\lambda \in \Pi(\overline{\mathfrak{R}})$. Either λ or $-\lambda$ is represented by a holomorphic curve class, but not both. Thus, only some of the weights of \mathfrak{R} will be identified via Gromov-Witten invariants. Nevertheless, the analysis outlined in the introduction to this subsection will find non-zero invariants for all classes $\phi_{\mathbb{Q}}(\Pi(\mathfrak{R}))$. Note that this is required by CPT: the representation content of a hypermultiplet associated to a complex representation is $\mathfrak{R} \oplus \overline{\mathfrak{R}}$. Thus, holomorphic and anti-holomorphic curves combined must furnish this reducible representation. It follows that the holomorphic curves in $S(\mathfrak{R}) \cup S(\overline{\mathfrak{R}})$ combined must yield precisely the elements of $\Pi(\mathfrak{R})$.

If \mathfrak{R} is self-conjugate, then $\lambda \in \Pi(\mathfrak{R}) \leftrightarrow -\lambda \in \Pi(\mathfrak{R})$. Again, either λ or $-\lambda$ is represented by a holomorphic curve class, but not both. The analysis outlined above applied to this situation will therefore only find part of $\Pi(\mathfrak{R})$ represented by classes in N_1 with non-zero Gromov-Witten invariants. Note that when \mathfrak{R} is self-conjugate, CPT does not dictate the doubling of degrees of freedom for hypermultiplets: half-hypermultiplets are permitted.

To summarize, these considerations entail the following for the book keeping of matter content: if \mathfrak{R} is complex, an isolated curve and its complex conjugate give rise to a field and its conjugate in a hypermultiplet, the corresponding Gromov-Witten invariant hence allows us to read off the number of hypermultiplets. If \mathfrak{R} is self-conjugate, an isolated curve and its complex conjugate give rise to different fields in a half-hypermultiplet, the Gromov-Witten invariant hence counts the number of half-hypermultiplets.

The distribution of holomorphic vs. holomorphic curves in $S(\mathfrak{R})$ changes under flops. It thus differs among the elements in $(\mathfrak{g})_n$.

5.2.2 When roots and weights coincide

The deduction of field content from Gromov-Witten invariants requires additional care when some weights and roots coincide. This happens e.g. when the vector representation contains at least one zero weight (this happens iff the highest weight of the vector representation is an element of the root lattice), as by

$$\mathbf{vec} \otimes \overline{\mathbf{vec}} = \mathbf{1} \oplus \mathbf{adj} \oplus \mathbf{sym}, \quad (5.2)$$

all weights of the vector representation are contained in the set of roots in this case. In particular, this happens for the Lie algebras B_n, F_4, G_2 .

In the case of $(G_2)_3$, e.g., the image of only half of the simple roots arises in $N_1(X)$ with Gromov-Witten invariant -2. No other classes with vanishing $[C_B]$, $[C_F]$, and $[C_{r_0}]$ components have non-vanishing Gromov-Witten invariant. The interpretation is that a hypermultiplet in the real vector representation $\mathbf{7}$ is present. The holomorphic curve classes in $\phi_{\mathbb{Q}}(\Pi(\mathbf{7}))$ contribute +2 to the Gromov-Witten invariants of the classes ($\mathbf{7}$ is self-conjugate \rightarrow a contribution of +2 to the Gromov-Witten invariant implies 2 half-hypermultiplets). As

all of the weights of the **7** representations coincide with simple roots of G_2 , the net effect of the presence of such curves is to cancel the Gromov-Witten invariants of certain simple roots.

5.2.3 Matter curves and the toric Mori cone

Representations \mathfrak{R} whose weights do not lie in Λ^{root} can leave an imprint on the generators of the toric Mori cone. When the toric Mori cone is smooth, we find that its generators can be expressed in terms of the distinguished curve classes introduced in section 3.7 as follows: three are linear combinations of the classes $[C_B]$, $[C_F]$, and $[C_{r_0}]$, and $\text{rank}(\mathfrak{g})$ are linear combinations of the classes of the curves C_{r_i} . These latter linear combinations correspond either to simple roots of \mathfrak{g} or to weights in a representation \mathfrak{R} (or either \mathfrak{R} or $\overline{\mathfrak{R}}$, for complex representations) of \mathfrak{g} . Unlike the naive expectation but in agreement with the discussion in section 5.2.1, the weights that occur are not the highest weight of \mathfrak{R} (or $\overline{\mathfrak{R}}$), hence the image under $\phi_{\mathbb{Q}}$ of the weights of \mathfrak{R} (or $\overline{\mathfrak{R}}$) does not lie in the toric Mori cone. However, for all weights $\lambda \in \Pi(\mathfrak{R})$ not mapped into the toric Mori cone, $-\lambda$ is. Which weights occur in the toric Mori cone depends on the choice of hypersurface in the birational equivalence class $(\mathfrak{g})_n$.

In the case of varieties whose toric Mori cones are smooth, the presence of matter curves associated to representations \mathfrak{R} for which $\Pi(\mathfrak{R}) \not\subset \Lambda^{root}$ can hence be inferred from a generator whose preimage under $\phi_{\mathbb{Q}}$ lies in $\Pi(\mathfrak{R})$. In the case of $(E_6)_n$ and $(E_7)_n$, we can even determine the multiplicity with which \mathfrak{R} occurs: at least one of the generator in question occurs as an irreducible component of the intersection of a torus invariant surface of the ambient space with X . The multiplicity of this reducible intersection coincides with the multiplicity of \mathfrak{R} . It would be interesting to study the systematics underlying this observation further.

Example of toric Mori cone: $(E_6)_3$ We consider a variety X of embedding type I in $(E_6)_3$. In table 5.1, we give the generators of the toric Mori cone in terms of the classes of distinguished curves whose Mori vectors are listed in table 3.3. We note that $\phi_{\mathbb{Q}}^{-1}$ maps C_1 , C_2 , C_3 to simple roots of E_6 , C_4 and C_6 to weights of the **27** representation, and C_5 to a weight of the $\overline{\mathbf{27}}$ representation.

Furthermore, $3C_4 = [D_{r_2}^X \cdot D_{r_5}^X]$, and $3C_5 = [D_{r_1}^X \cdot D_{r_6}^X]$, 3 being the number of hypermultiplets in the **27** representation which arise upon compactification on X .

Acknowledgements

We are grateful to Michele Del Zotto, Albrecht Klemm, Guglielmo Lockhart and Timo Weigand for discussions.

	C_{r_1}	C_{r_2}	C_{r_3}	C_{r_4}	C_{r_5}	C_{r_6}	C_{r_0}	C_F	C_B
C_1	0	0	1	0	0	0	0	0	0
C_2	0	0	0	1	0	0	0	0	0
C_3	0	0	0	0	1	0	0	0	0
C_4	$-\frac{1}{3}$	$\frac{1}{3}$	0	0	$-\frac{1}{3}$	$\frac{1}{3}$	0	0	0
C_5	$\frac{1}{3}$	$-\frac{1}{3}$	0	0	$\frac{1}{3}$	$\frac{2}{3}$	0	0	0
C_6	$\frac{2}{3}$	$\frac{1}{3}$	0	0	$-\frac{1}{3}$	$-\frac{2}{3}$	0	0	0
C_7	0	0	0	0	0	0	1	0	0
C_8	0	0	0	0	0	0	0	1	0
C_9	0	0	0	0	0	0	-1	0	1

Table 5.1: Generators of the toric Mori cone for $(E_6)_3$ expressed in terms of the Mori vectors of the distinguished curves listed in table 3.3.

A Assorted data on the birational equivalence classes $(\mathfrak{g})_n$

In this appendix, we record some toric data of the geometries we have studied in this paper, notably the generators of the toric Mori cones. To keep this section within a reasonable length, we discuss only the first two members of the A - and B -series, and after the first example, $(A_2)_n$, refrain from listing data of varieties of embedding type II (except for the case $(A_2)_3$, where the only element is of this type).

A.1 A -series

A_2

Occurs over Hirzebruch bases \mathbb{F}_n , $n = 0, \dots, 3$.

Additional 1-cones:

$$\begin{aligned} u_{\rho_{r_1}} &= (-1 \ -1 \ 0 \ -1) \\ u_{\rho_{r_2}} &= (-1 \ -2 \ 0 \ -1) \end{aligned} \tag{A.1}$$

Matter content: $6(3 - n)$ hypermultiplets in the complex representation $\mathbf{3}$.

For $n = 0, \dots, 2$, $(A_2)_n$ contains exactly one variety of embedding type I. The corresponding toric Mori cones coincide and are smooth. Their generators are given in table A.1. The curve C_2 corresponds to a weights of the representation $\mathbf{3}$.

In addition, $(A_2)_n$ for $n = 1, 3$ also contains a variety of embedding type II. For $n = 3$, this is the only variety contained in $(A_2)_n$. The corresponding toric Mori cones are smooth. Their

	C_{r_1}	C_{r_2}	C_{r_0}	C_F	C_B
C_1	0	1	0	0	0
C_2	$\frac{1}{3}$	$-\frac{1}{3}$	0	0	0
C_3	0	0	1	0	0
C_4	0	0	0	1	0
C_5	0	0	0	0	1

Table A.1: The generators of the toric Mori cone of the $(A_2)_n$ varieties of embedding type I.

generators, expressed in terms of the Mori vectors of the distinguished curves introduced in section 3.7 for the case that $u * v \notin I_{\text{Stanley-Reisner}}(Y)$ are given in table A.2.

	C_{r_1}	C_{r_2}	C_{r_0}	C_F	C_B		C_{r_1}	C_{r_2}	C_{r_0}	C_F	C_B	
C_1	0	1	0	0	0		C_1	0	1	-1	0	1
C_2	$\frac{1}{3}$	$-\frac{1}{3}$	0	0	0		C_2	$\frac{1}{3}$	$-\frac{1}{3}$	0	0	0
C_3	0	0	1	0	-1		C_3	0	0	1	0	-1
C_4	0	0	0	1	-1		C_4	0	0	0	1	0
C_5	0	0	0	0	1		C_5	0	0	0	0	1

Table A.2: The generators of the toric Mori cone ($n = 1$ on the left, $n = 2$ on the right) of the $(A_2)_n$ varieties of embedding type II.

A_3

Occurs over Hirzebruch bases \mathbb{F}_n , $n = 0, \dots, 2$.

Additional 1-cones:

$$\begin{aligned}
u_{\rho_{r_1}} &= (-1 \quad -1 \quad 0 \quad -1) \\
u_{\rho_{r_2}} &= (0 \quad -1 \quad 0 \quad -1) \\
u_{\rho_{r_3}} &= (-1 \quad -2 \quad 0 \quad -1)
\end{aligned} \tag{A.2}$$

Matter content:

- $(A_3)_1$: 12 hypermultiplets in the complex representation **4**, 2 half hypermultiplets in the self-conjugate representation **6**.
- $(A_3)_2$: 8 hypermultiplets in the complex representation **4**.

For $n = 0, 1, 2$, $(A_3)_n$ contains exactly one variety of embedding type I. The corresponding toric Mori cones coincide and are smooth. Their generators are given in table A.3. Curves corresponding to weights of the representation **4** are highlighted in red, and those corresponding to the representation **6** in green.

In addition, $(A_3)_1$ also contains an embedding type II variety.

	C_{r_1}	C_{r_2}	C_{r_3}	C_{r_0}	C_F	C_B
C_1	0	0	1	0	0	0
C_2	$-\frac{1}{4}$	$\frac{1}{2}$	$\frac{1}{4}$	0	0	0
C_3	$\frac{1}{2}$	0	$-\frac{1}{2}$	0	0	0
C_4	0	0	0	1	0	0
C_5	0	0	0	0	1	0
C_6	0	0	0	0	0	1

Table A.3: The generators of the toric Mori cone of the $(A_3)_n$ varieties of embedding type I.

A.2 B -series

B_3

Occurs over Hirzebruch bases \mathbb{F}_n , $n = 0, \dots, 3$.

Additional 1-cones:

$$\begin{aligned}
u_{\rho_{r_1}} &= (0 \quad -1 \quad 0 \quad -1) \\
u_{\rho_{r_2}} &= (-2 \quad -3 \quad 0 \quad -2) \\
u_{\rho_{r_3}} &= (-1 \quad -1 \quad 0 \quad -1)
\end{aligned} \tag{A.3}$$

Matter content:

- $2 * (3 - n)$ half-hypermultiplets in the self-conjugate representation **7**.
- $2 * 2(4 - n)$ half-hypermultiplets in the self-conjugate representation **8**.

For all $n = 0, \dots, 3$, $(B_3)_n$ contains exactly one variety of embedding type I. The corresponding toric Mori cones are smooth. They have six generators, five of which are independent of n , given in table A.4. The curve C_3 corresponds to a weight in the representation **8**.

	C_{r_1}	C_{r_2}	C_{r_3}	C_{r_0}	C_F	C_B
C_1	0	1	0	0	0	0
C_2	0	0	1	0	0	0
C_3	$\frac{1}{2}$	0	$-\frac{1}{2}$	0	0	0
C_4	0	0	0	1	0	0
C_5	0	0	0	0	1	0

	C_{r_1}	C_{r_2}	C_{r_3}	C_{r_0}	C_F	C_B
$(C_6)_{0,1,2}$	0	0	0	0	0	1
$(C_6)_3$	0	0	0	-1	0	1

Table A.4: The five n -independent generator of the toric Mori cone of the varieties in $(B_3)_n$ of embedding type I given on the left, and the last n -dependent generator given on the right.

In addition, $(B_3)_n$ for $n = 1, 3$ also contains a variety of embedding type II.

Note that all the weights of the representation **7** are also roots. The associated Gromov-Witten invariants at base \mathbb{F}_n are thus $2 * (3 - n) - 2 = 4 - 2n$. In particular, at $n = 2$, the contributions from roots and weights cancel.

B_4

Occurs over Hirzebruch bases \mathbb{F}_n , $n = 0, \dots, 4$.

Additional 1-cones:

$$\begin{aligned}
 u_{\rho_{r_1}} &= (-1 \quad -1 \quad 0 \quad -1) \\
 u_{\rho_{r_2}} &= (2 \quad -3 \quad 0 \quad -2) \\
 u_{\rho_{r_3}} &= (-1 \quad -2 \quad 0 \quad -2) \\
 u_{\rho_{r_4}} &= (0 \quad -1 \quad 0 \quad -1)
 \end{aligned} \tag{A.4}$$

Matter content:

- $2 * (5 - n)$ half-hypermultiplets in the self-conjugate representation **9**.
- $2 * (4 - n)$ half-hypermultiplets in the self-conjugate representation **16**.

For all $n = 0, \dots, 4$, $(B_4)_n$ contains exactly one variety of embedding type I. The corresponding toric Mori cones are smooth. They have seven generators, six of which are independent of n , given in table A.5. The curve C_4 corresponds to a weight in the representation **16**.

	C_{r_1}	C_{r_2}	C_{r_3}	C_{r_4}	C_{r_0}	C_F	C_B
C_1	1	0	0	0	0	0	0
C_2	0	1	0	0	0	0	0
C_3	0	0	0	1	0	0	0
C_4	$-\frac{1}{2}$	0	$\frac{1}{2}$	0	0	0	0
C_5	0	0	0	0	1	0	0
C_6	0	0	0	0	0	1	0

	C_{r_1}	C_{r_2}	C_{r_3}	C_{r_4}	C_{r_0}	C_F	C_B
$(C_6)_{0,1,2}$	0	0	0	0	0	0	1
$(C_6)_3$	0	0	0	0	-1	0	1
$(C_6)_4$	0	0	0	0	-2	0	1

Table A.5: The six n -independent generator of the toric Mori cone of the $(B_4)_n$ varieties of embedding type I given on the left, and the last n -dependent generator given on the right.

In addition, $(B_4)_n$ for $n = 1, 3$ also contains a variety of embedding type II.

Note that all the weights of the representation **9** are also roots. The associated Gromov-Witten invariants at base \mathbb{F}_n are thus $2 * (5 - n) - 2 = 2(4 - n)$. These Gromov-Witten invariants hence coincide with those associated to the **16** representation. At $n = 4$, the contributions associated to the weights of the representation **9** cancels against that of roots.

A.3 D -series

D_5

Occurs over Hirzebruch bases \mathbb{F}_n , $n = 0, \dots, 4$.

Additional 1-cones:

$$\begin{aligned}
u_{\rho_{r_1}} &= (-1 \ -1 \ 0 \ -1) \\
u_{\rho_{r_2}} &= (-2 \ -3 \ 0 \ -2) \\
u_{\rho_{r_3}} &= (-1 \ -2 \ 0 \ -2) \\
u_{\rho_{r_4}} &= (0 \ -1 \ 0 \ -1) \\
u_{\rho_{r_5}} &= (0 \ 0 \ 0 \ -1)
\end{aligned} \tag{A.5}$$

Matter content:

- $2 * (6 - n)$ half-hypermultiplets in the self-conjugate representation **10**.
- $(4 - n)$ hypermultiplets in the complex representation **16**.

For $n = 0, \dots, 3$, $(D_5)_n$ contains three varieties of embedding type I. The corresponding toric Mori cones are smooth. They have eight generators, given in table A.6. Curves corresponding to weights of the representation **10** are highlighted in blue, those of the representation **16** in green, and those of the representation **16** in red.

	C_{r_1}	C_{r_2}	C_{r_3}	C_{r_4}	C_{r_5}	C_{r_0}	C_F	C_B
C_1	0	1	0	0	0	0	0	0
C_2	0	0	0	1	0	0	0	0
C_3	$-\frac{1}{2}$	0	$\frac{1}{2}$	$-\frac{1}{4}$	$\frac{1}{4}$	0	0	0
C_4	$\frac{1}{2}$	0	$\frac{1}{2}$	$\frac{1}{4}$	$-\frac{1}{4}$	0	0	0
C_5	$\frac{1}{2}$	0	$-\frac{1}{2}$	$-\frac{1}{4}$	$\frac{1}{4}$	0	0	0
C_6	0	0	0	0	0	1	0	0
C_7	0	0	0	0	0	0	1	0

	C_{r_1}	C_{r_2}	C_{r_3}	C_{r_4}	C_{r_5}	C_{r_0}	C_F	C_B
C_1	1	0	0	0	0	0	0	0
C_2	0	0	1	0	0	0	0	0
C_3	0	0	0	1	0	0	0	0
C_4	$\frac{1}{2}$	1	$\frac{1}{2}$	$\frac{1}{4}$	$-\frac{1}{4}$	0	0	0
C_5	$-\frac{1}{2}$	0	$-\frac{1}{2}$	$-\frac{1}{4}$	$\frac{1}{4}$	0	0	0
C_6	0	0	0	0	0	1	0	0
C_7	0	0	0	0	0	0	1	0

	C_{r_1}	C_{r_2}	C_{r_3}	C_{r_4}	C_{r_5}	C_{r_0}	C_F	C_B
C_1	1	0	0	0	0	0	0	0
C_2	0	1	0	0	0	0	0	0
C_3	0	0	0	1	0	0	0	0
C_4	$-\frac{1}{2}$	0	$\frac{1}{2}$	$\frac{1}{4}$	$-\frac{1}{4}$	0	0	0
C_5	0	0	0	$-\frac{1}{2}$	$\frac{1}{2}$	0	0	0
C_6	0	0	0	0	0	1	0	0
C_7	0	0	0	0	0	0	1	0

	C_{r_1}	C_{r_2}	C_{r_3}	C_{r_4}	C_{r_5}	C_{r_0}	C_F	C_B
$(C_8)_{0,1,2}$	0	0	0	0	0	0	0	1
$(C_8)_3$	0	0	0	0	0	-1	0	1

Table A.6: Generators of the toric Mori cones for the three $(D_5)_n$ varieties of embedding type I for $n = 0, \dots, 3$, expressed in terms of the Mori vectors of the distinguished curves introduce in section 3.6. Only the generator C_8 depends on the base surface \mathbb{F}_n , but its expression in terms of the distinguished curves coincides for all three $(D_5)_n$ varieties of embedding type I. The corresponding classes are denoted as $(C_8)_n$ in the last table.

In addition, $(D_5)_n$ for $n = 1, 3$ also contain three varieties of embedding type II.

The class $(D_5)_4$ contains a single variety. Its toric Mori cone, given in table A.7, is not simplicial.

	C_{r_1}	C_{r_2}	C_{r_3}	C_{r_4}	C_{r_5}	C_{r_0}	C_F	C_B
C_1	0	1	0	0	0	0	0	0
C_1	0	0	1	0	0	0	0	0
C_3	0	0	0	1	0	0	0	0
C_4	0	0	0	0	1	0	0	0
C_5	$\frac{1}{4}$	$\frac{1}{2}$	0	$-\frac{1}{4}$	$-\frac{1}{2}$	0	0	0
C_6	$-\frac{1}{4}$	$\frac{1}{2}$	1	$\frac{1}{4}$	$\frac{1}{2}$	0	0	0
C_7	$\frac{1}{2}$	0	0	$-\frac{1}{2}$	0	0	0	0
C_8	0	0	0	0	0	1	0	0
C_9	0	0	0	0	0	0	1	0
C_{10}	0	0	0	0	0	-2	0	1

Table A.7: Generators of the non-simplicial toric Mori cone for the unique $(D_5)_5$ variety.

A.4 E_6

Occurs over Hirzebruch bases \mathbb{F}_n , $n = 0, \dots, 6$.

Additional 1-cones:

$$\begin{aligned}
u_{\rho_{r_1}} &= (0 & 0 & 0 & -1) \\
u_{\rho_{r_2}} &= (-1 & -1 & 0 & -2) \\
u_{\rho_{r_3}} &= (-2 & -3 & 0 & -3) \\
u_{\rho_{r_4}} &= (-1 & -2 & 0 & -2) \\
u_{\rho_{r_5}} &= (0 & -1 & 0 & -1) \\
u_{\rho_{r_6}} &= (-2 & -3 & 0 & -2)
\end{aligned} \tag{A.6}$$

Matter content: $6 - n$ hypermultiplets in the complex representation **27**.

The cases $n = 0, \dots, 5$ are similar: there are 4 varieties in $(E_6)_n$ of embedding type I. All corresponding toric Mori cones are smooth. They are given in table A.8 in terms of the classes of distinguished curves given in section 3.7. Weights of the representation **27** are highlighted in green, those of the representation $\overline{\mathbf{27}}$ in red.

In addition, $(E_6)_n$ for $n = 1, 3, 5$ contains four varieties of embedding type II.

The class $(E_6)_6$ contains a single variety, compactification on which gives rise to a theory without charged matter. Its toric Mori cone, given in table A.9, is not simplicial.

	C_{r_1}	C_{r_2}	C_{r_3}	C_{r_4}	C_{r_5}	C_{r_6}	C_{r_0}	C_F	C_B		C_{r_1}	C_{r_2}	C_{r_3}	C_{r_4}	C_{r_5}	C_{r_6}	C_{r_0}	C_F	C_B	
C_1	0	0	1	0	0	0	0	0	0	C_1	1	0	0	0	0	0	0	0	0	0
C_2	0	0	0	1	0	0	0	0	0	C_2	0	0	1	0	0	0	0	0	0	0
C_3	0	0	0	0	0	1	0	0	0	C_3	0	0	0	1	0	0	0	0	0	0
C_4	$-\frac{1}{3}$	$\frac{1}{3}$	0	$-\frac{1}{3}$	$\frac{1}{3}$	0	0	0	0	C_4	0	0	0	0	1	0	0	0	0	0
C_5	$\frac{1}{3}$	$-\frac{1}{3}$	0	$\frac{1}{3}$	$\frac{2}{3}$	0	0	0	0	C_5	0	0	0	0	0	1	0	0	0	0
C_6	$\frac{2}{3}$	$\frac{1}{3}$	0	$-\frac{1}{3}$	$-\frac{2}{3}$	0	0	0	0	C_6	$-\frac{1}{3}$	$\frac{1}{3}$	0	$-\frac{1}{3}$	$-\frac{2}{3}$	0	0	0	0	0
C_7	0	0	0	0	0	0	1	0	0	C_7	0	0	0	0	0	0	1	0	0	0
C_8	0	0	0	0	0	0	0	1	0	C_8	0	0	0	0	0	0	0	1	0	0

	C_{r_1}	C_{r_2}	C_{r_3}	C_{r_4}	C_{r_5}	C_{r_6}	C_{r_0}	C_F	C_B		C_{r_1}	C_{r_2}	C_{r_3}	C_{r_4}	C_{r_5}	C_{r_6}	C_{r_0}	C_F	C_B	
C_1	0	0	1	0	0	0	0	0	0	C_1	0	1	0	0	0	0	0	0	0	0
C_2	0	0	0	0	1	0	0	0	0	C_2	0	0	0	1	0	0	0	0	0	0
C_3	0	0	0	0	0	1	0	0	0	C_3	0	0	0	0	1	0	0	0	0	0
C_4	$\frac{1}{3}$	$-\frac{1}{3}$	0	$\frac{1}{3}$	$-\frac{1}{3}$	0	0	0	0	C_4	0	0	0	0	0	1	0	0	0	0
C_5	$-\frac{1}{3}$	$\frac{1}{3}$	0	$\frac{2}{3}$	$\frac{1}{3}$	0	0	0	0	C_5	$\frac{1}{3}$	$-\frac{1}{3}$	0	$-\frac{2}{3}$	$-\frac{1}{3}$	0	0	0	0	0
C_6	$\frac{1}{3}$	$\frac{2}{3}$	0	$-\frac{2}{3}$	$-\frac{1}{3}$	0	0	0	0	C_6	$-\frac{1}{3}$	$\frac{1}{3}$	1	$\frac{2}{3}$	$\frac{1}{3}$	0	0	0	0	0
C_7	0	0	0	0	0	0	1	0	0	C_7	0	0	0	0	0	0	1	0	0	0
C_8	0	0	0	0	0	0	0	1	0	C_8	0	0	0	0	0	0	0	1	0	0

	C_{r_1}	C_{r_2}	C_{r_3}	C_{r_4}	C_{r_5}	C_{r_6}	C_{r_0}	C_F	C_B
$(C_9)_{0,1,2}$	0	0	0	0	0	0	0	0	1
$(C_9)_3$	0	0	0	0	0	0	-1	0	1
$(C_9)_4$	0	0	0	0	0	0	-2	0	1
$(C_9)_5$	0	0	0	0	0	-1	-3	0	1

Table A.8: Generators of the toric Mori cones for the four $(E_6)_n$ varieties of embedding type I in terms of the Mori vectors of the distinguished curves listed in table 3.3. Only the generator C_9 depends on the base surface \mathbb{F}_n , but its expression in terms of the distinguished curves coincides for all four $(E_6)_n$ varieties of embedding type I. The corresponding classes are denoted as $(C_9)_n$ in the last table.

	C_{r_1}	C_{r_2}	C_{r_3}	C_{r_4}	C_{r_5}	C_{r_6}	C_{r_0}	C_F	C_B
C_1	1	0	0	0	0	0	0	0	0
C_2	0	1	0	0	0	0	0	0	0
C_3	0	0	1	0	0	0	0	0	0
C_4	0	0	0	1	0	0	0	0	0
C_5	0	0	0	0	1	0	0	0	0
C_6	0	0	0	0	0	1	0	0	0
C_7	$-\frac{1}{3}$	$\frac{1}{3}$	1	$\frac{2}{3}$	$\frac{1}{3}$	0	0	0	0
C_8	$\frac{2}{3}$	$\frac{1}{3}$	0	$-\frac{1}{3}$	$-\frac{2}{3}$	0	0	0	0
C_9	$\frac{1}{3}$	$\frac{2}{3}$	0	$-\frac{2}{3}$	$-\frac{1}{3}$	0	0	0	0
C_{10}	0	0	0	0	0	0	1	0	0
C_{11}	0	0	0	0	0	0	0	1	0
C_{12}	0	0	0	0	0	-2	-4	0	1

Table A.9: Generators of the non-simplicial toric Mori cone for the unique $(E_6)_6$ variety.

A.5 E_7

Occurs over Hirzebruch bases \mathbb{F}_n , $n = 0, \dots, 8$.

Additional 1-cones:

$$\begin{aligned}
 u_{\rho_{r_1}} &= (-2 & -3 & 0 & -2) \\
 u_{\rho_{r_2}} &= (-2 & -3 & 0 & -3) \\
 u_{\rho_{r_3}} &= (-2 & -3 & 0 & -4) \\
 u_{\rho_{r_4}} &= (-1 & -2 & 0 & -3) \\
 u_{\rho_{r_5}} &= (0 & -1 & 0 & -2) \\
 u_{\rho_{r_6}} &= (0 & 0 & 0 & -1) \\
 u_{\rho_{r_7}} &= (-1 & -1 & 0 & -2)
 \end{aligned} \tag{A.7}$$

Matter content: $8 - n$, $n = 0, \dots, 8$, half-hypermultiplets in the self-conjugate representation **56**.

For $n = 0, \dots, 8$, $(E_7)_n$ contains 4 varieties of embedding type I. All corresponding toric Mori cones except for $n = 8$ are smooth. The generators for $n = 0, \dots, 7$ are given in table A.10 in terms of the classes of distinguished curves given in section 3.7. Curves corresponding to weights of the representation **56** are discernible.

In addition, $(E_7)_n$ for $n = 1, 3, 5, 7$ contains four varieties of embedding type II.

The class $(E_7)_8$ contains a single variety, compactification on which gives rise to a theory without charged matter. Its toric Mori cone, given in table A.11, is not simplicial.

A.6 E_8

Occurs over Hirzebruch base \mathbb{F}_{12}

Additional 1-cones:

$$\begin{aligned}
 u_{\rho_{r_1}} &= (0 & -1 & 0 & -2) \\
 u_{\rho_{r_2}} &= (-1 & -2 & 0 & -4) \\
 u_{\rho_{r_3}} &= (-2 & -3 & 0 & -6) \\
 u_{\rho_{r_4}} &= (-2 & -3 & 0 & -5) \\
 u_{\rho_{r_5}} &= (-2 & -3 & 0 & -4) \\
 u_{\rho_{r_6}} &= (-2 & -3 & 0 & -3) \\
 u_{\rho_{r_7}} &= (-2 & -3 & 0 & -2) \\
 u_{\rho_{r_8}} &= (-1 & -1 & 0 & -3)
 \end{aligned} \tag{A.8}$$

	C_{r_1}	C_{r_2}	C_{r_3}	C_{r_4}	C_{r_5}	C_{r_6}	C_{r_7}	C_{r_0}	C_F	C_B		C_{r_1}	C_{r_2}	C_{r_3}	C_{r_4}	C_{r_5}	C_{r_6}	C_{r_7}	C_{r_0}	C_F	C_B	
C_1	1	0	0	0	0	0	0	0	0	0	C_1	1	0	0	0	0	0	0	0	0	0	
C_2	0	1	0	0	0	0	0	0	0	0	C_1	0	1	0	0	0	0	0	0	0	0	0
C_3	0	0	1	0	0	0	0	0	0	0	C_3	0	0	1	0	0	0	0	0	0	0	0
C_4	0	0	0	0	1	0	0	0	0	0	C_4	0	0	0	0	1	0	0	0	0	0	0
C_5	0	0	0	$\frac{1}{2}$	0	$-\frac{1}{2}$	$\frac{1}{2}$	0	0	0	C_5	0	0	0	0	0	1	0	0	0	0	0
C_6	0	0	0	$\frac{1}{2}$	0	$\frac{1}{2}$	$-\frac{1}{2}$	0	0	0	C_6	0	0	0	0	0	0	1	0	0	0	0
C_7	0	0	0	$-\frac{1}{2}$	0	$\frac{1}{2}$	$\frac{1}{2}$	0	0	0	C_7	0	0	0	$\frac{1}{2}$	0	$-\frac{1}{2}$	$-\frac{1}{2}$	0	0	0	0
C_8	0	0	0	0	0	0	0	1	0	0	C_8	0	0	0	0	0	0	0	1	0	0	0
C_9	0	0	0	0	0	0	0	0	1	0	C_9	0	0	0	0	0	0	0	0	1	0	0

	C_{r_1}	C_{r_2}	C_{r_3}	C_{r_4}	C_{r_5}	C_{r_6}	C_{r_7}	C_{r_0}	C_F	C_B		C_{r_1}	C_{r_2}	C_{r_3}	C_{r_4}	C_{r_5}	C_{r_6}	C_{r_7}	C_{r_0}	C_F	C_B	
C_1	1	0	0	0	0	0	0	0	0	0	C_1	1	0	0	0	0	0	0	0	0	0	
C_2	0	1	0	0	0	0	0	0	0	0	C_2	0	1	0	0	0	0	0	0	0	0	0
C_3	0	0	1	0	0	0	0	0	0	0	C_3	0	0	0	1	0	0	0	0	0	0	0
C_4	0	0	0	1	0	0	0	0	0	0	C_4	0	0	0	0	1	0	0	0	0	0	0
C_5	0	0	0	0	0	1	0	0	0	0	C_5	0	0	0	0	0	0	1	0	0	0	0
C_6	0	0	0	$-\frac{1}{2}$	0	$-\frac{1}{2}$	$\frac{1}{2}$	0	0	0	C_6	0	0	0	$-\frac{1}{2}$	0	$\frac{1}{2}$	$-\frac{1}{2}$	0	0	0	0
C_7	0	0	0	$\frac{1}{2}$	1	$\frac{1}{2}$	$-\frac{1}{2}$	0	0	0	C_7	0	0	1	$\frac{1}{2}$	0	$-\frac{1}{2}$	$\frac{1}{2}$	0	0	0	0
C_8	0	0	0	0	0	0	0	1	0	0	C_8	0	0	0	0	0	0	0	1	0	0	0
C_9	0	0	0	0	0	0	0	0	1	0	C_9	0	0	0	0	0	0	0	0	1	0	0

	C_{r_1}	C_{r_2}	C_{r_3}	C_{r_4}	C_{r_5}	C_{r_6}	C_{r_7}	C_{r_0}	C_F	C_B
$(C_{10})_{0,1,2}$	0	0	0	0	0	0	0	0	0	1
$(C_{10})_3$	0	0	0	0	0	0	0	-1	0	1
$(C_{10})_4$	0	0	0	0	0	0	0	-2	0	1
$(C_{10})_5$	-1	0	0	0	0	0	0	-3	0	1
$(C_{10})_6$	-2	0	0	0	0	0	0	-4	0	1
$(C_{10})_7$	-3	-1	0	0	0	0	0	-5	0	1

Table A.10: Generators of the toric Mori cones for the four $(E_7)_n$ varieties of embedding type I for $n = 0, \dots, 7$, expressed in terms of the Mori vectors of the distinguished curves introduce in section 3.6. Only the generator C_{10} depends on the base surface \mathbb{F}_n , but its expression in terms of the distinguished curves coincides for all four $(E_7)_n$ varieties of embedding type I. The corresponding classes are denoted as $(C_{10})_n$ in the last table.

Matter content: none.

$(E_8)_{12}$ contains exactly one variety. It is of embedding type I. Its toric Mori vector is smooth. Its generators are given in table A.12 in terms of the classes of distinguished curves given in section 3.7.

A.7 F_4

Occurs over Hirzebruch bases \mathbb{F}_n , $n = 0, \dots, 5$.

	C_{r_1}	C_{r_2}	C_{r_3}	C_{r_4}	C_{r_5}	C_{r_6}	C_{r_7}	C_{r_0}	C_F	C_B
C_1	1	0	0	0	0	0	0	0	0	0
C_2	0	1	0	0	0	0	0	0	0	0
C_3	0	0	1	0	0	0	0	0	0	0
C_4	0	0	0	1	0	0	0	0	0	0
C_5	0	0	0	0	1	0	0	0	0	0
C_6	0	0	0	0	0	1	0	0	0	0
C_7	0	0	0	0	0	0	1	0	0	0
C_8	0	0	0	$\frac{1}{2}$	1	$\frac{1}{2}$	$-\frac{1}{2}$	0	0	0
C_9	0	0	1	$\frac{1}{2}$	0	$-\frac{1}{2}$	$\frac{1}{2}$	0	0	0
C_{10}	0	0	0	0	0	0	0	1	0	0
C_{11}	0	0	0	0	0	0	0	0	1	0
C_{12}	-4	-2	0	0	0	0	0	-6	0	1

Table A.11: Generators of the non-simplicial toric Mori cone for the unique $(E_7)_8$ variety.

	C_{r_1}	C_{r_2}	C_{r_3}	C_{r_4}	C_{r_5}	C_{r_6}	C_{r_7}	C_{r_8}	C_{r_0}	C_F	C_B
C_1	1	0	0	0	0	0	0	0	0	0	0
C_2	0	1	0	0	0	0	0	0	0	0	0
C_3	0	0	1	0	0	0	0	0	0	0	0
C_4	0	0	0	1	0	0	0	0	0	0	0
C_5	0	0	0	0	1	0	0	0	0	0	0
C_6	0	0	0	0	0	1	0	0	0	0	0
C_7	0	0	0	0	0	0	1	0	0	0	0
C_8	0	0	0	0	0	0	0	1	0	0	0
C_9	0	0	0	0	0	0	0	0	1	0	0
C_{10}	0	0	0	0	0	0	0	0	0	1	0
C_{11}	0	0	0	0	-2	-4	-6	-8	0	-10	0

Table A.12: Generators of the toric Mori cone of the sole variety contained in $(E_8)_{12}$.

Additional 1-cones:

$$\begin{aligned}
u_{\rho_{r_1}} &= (-2 \quad -3 \quad 0 \quad -2) \\
u_{\rho_{r_2}} &= (-2 \quad -3 \quad 0 \quad -3) \\
u_{\rho_{r_3}} &= (-1 \quad -2 \quad 0 \quad -2) \\
u_{\rho_{r_4}} &= (0 \quad -1 \quad 0 \quad -1)
\end{aligned} \tag{A.9}$$

Matter content: $2 * (5 - n)$ half-hypermultiplets in the self-conjugate representation **26**.

For all $n = 0, \dots, 5$, $(F_4)_n$ contains exactly one variety of embedding type I. The corresponding toric Mori cones are smooth. They have seven generators. The classes of six of these are given by $[C_{r_1}], \dots, [C_{r_4}], [C_{r_0}], [C_F]$. The class of the last generator depends on n , and is given in table A.13.

In addition, $(F_4)_n$ for $n = 1, 3, 5$ also contains a variety of embedding type II.

Note that all weights of the **26** representation are also roots. The corresponding Gromov-

	C_{r_1}	C_{r_2}	C_{r_3}	C_{r_4}	C_{r_0}	C_F	C_B
$(C_7)_1$	0	0	0	0	0	0	1
$(C_7)_2$	0	0	0	0	0	0	1
$(C_7)_3$	0	0	0	0	-1	0	1
$(C_7)_4$	0	0	0	0	-2	0	1
$(C_7)_5$	-1	0	0	0	-3	0	1

Table A.13: The n -dependent generator of the toric Mori cone of the $(F_4)_n$ varieties of embedding type I.

Witten invariants at base \mathbb{F}_n are thus $2 * (5 - n) - 2$.

A.8 G_2

Occurs over Hirzebruch bases \mathbb{F}_n , $n = 0, \dots, 3$.

Additional 1-cones:

$$\begin{aligned} u_{\rho_{r_1}} &= (-1 \quad -1 \quad 0 \quad -1) \\ u_{\rho_{r_1}} &= (-2 \quad -3 \quad 0 \quad -2) \end{aligned} \tag{A.10}$$

Matter content: $2 * (7 - 2n)$ half-hypermultiplets in the self-conjugate representation **7**.

For all $n = 0, \dots, 3$, $(G_2)_n$ contains exactly one variety of embedding type I. The corresponding toric Mori cones are smooth. They have five generators. The classes of four of these are given by $[C_{r_1}], [C_{r_2}], [C_{r_0}], [C_F]$. The class of the last generator depends on n , and is given in table A.14.

	C_{r_1}	C_{r_2}	C_{r_0}	C_F	C_B
$(C_5)_1$	0	0	0	0	1
$(C_5)_2$	0	0	0	0	1
$(C_5)_3$	0	0	-1	0	1

Table A.14: The n -dependent generator of the toric Mori cone of the $(G_2)_n$ variety of embedding type I.

In addition, $(G_2)_n$ for $n = 1, 3$ also contains a variety of embedding type II.

Note that all weights of the **7** are also roots. The corresponding Gromov-Witten invariants at base \mathbb{F}_n are thus $2 * (7 - 2n) - 2 = 12 - 4n$. In particular, at $n = 3$, the contributions from roots and weights cancel.

References

- [1] C. Vafa, “Evidence for F theory,” *Nucl. Phys.* **B469** (1996) 403–418, [arXiv:hep-th/9602022](#) [hep-th].
- [2] D. R. Morrison and C. Vafa, “Compactifications of F theory on Calabi-Yau threefolds. 1,” *Nucl. Phys.* **B473** (1996) 74–92, [arXiv:hep-th/9602114](#) [hep-th].
- [3] D. R. Morrison and C. Vafa, “Compactifications of F theory on Calabi-Yau threefolds. 2.,” *Nucl. Phys.* **B476** (1996) 437–469, [arXiv:hep-th/9603161](#) [hep-th].
- [4] M. Bershadsky, K. A. Intriligator, S. Kachru, D. R. Morrison, V. Sadov, and C. Vafa, “Geometric singularities and enhanced gauge symmetries,” *Nucl. Phys.* **B481** (1996) 215–252, [arXiv:hep-th/9605200](#) [hep-th].
- [5] T. Weigand, “F-theory,” *PoS TASI2017* (2018) 016, [arXiv:1806.01854](#) [hep-th].
- [6] P. Candelas and A. Font, “Duality between the webs of heterotic and type II vacua,” *Nucl. Phys.* **B511** (1998) 295–325, [arXiv:hep-th/9603170](#) [hep-th].
- [7] E. Peralov and H. Skarke, “Enhanced gauged symmetry in type II and F theory compactifications: Dynkin diagrams from polyhedra,” *Nucl. Phys.* **B505** (1997) 679–700, [arXiv:hep-th/9704129](#) [hep-th].
- [8] S. H. Katz and C. Vafa, “Matter from geometry,” *Nucl. Phys.* **B497** (1997) 146–154, [arXiv:hep-th/9606086](#) [hep-th].
- [9] D. R. Morrison and W. Taylor, “Matter and singularities,” *JHEP* **01** (2012) 022, [arXiv:1106.3563](#) [hep-th].
- [10] A. Grassi and D. R. Morrison, “Anomalies and the Euler characteristic of elliptic Calabi-Yau threefolds,” *Commun. Num. Theor. Phys.* **6** (2012) 51–127, [arXiv:1109.0042](#) [hep-th].
- [11] J. J. Heckman, D. R. Morrison, and C. Vafa, “On the Classification of 6D SCFTs and Generalized ADE Orbifolds,” *JHEP* **05** (2014) 028, [arXiv:1312.5746](#) [hep-th]. [Erratum: *JHEP*06,017(2015)].
- [12] J. J. Heckman, D. R. Morrison, T. Rudelius, and C. Vafa, “Atomic Classification of 6D SCFTs,” *Fortsch. Phys.* **63** (2015) 468–530, [arXiv:1502.05405](#) [hep-th].
- [13] D. R. Morrison and W. Taylor, “Classifying bases for 6D F-theory models,” *Central Eur. J. Phys.* **10** (2012) 1072–1088, [arXiv:1201.1943](#) [hep-th].
- [14] G. Lockhart and C. Vafa, “Superconformal Partition Functions and Non-perturbative Topological Strings,” [arXiv:1210.5909](#) [hep-th].

- [15] J. Kim, S. Kim, K. Lee, J. Park, and C. Vafa, “Elliptic Genus of E-strings,” [arXiv:1411.2324 \[hep-th\]](#).
- [16] B. Haghighat, A. Klemm, G. Lockhart, and C. Vafa, “Strings of Minimal 6d SCFTs,” *Fortsch. Phys.* **63** (2015) 294–322, [arXiv:1412.3152 \[hep-th\]](#).
- [17] H.-C. Kim, S. Kim, and J. Park, “6d strings from new chiral gauge theories,” [arXiv:1608.03919 \[hep-th\]](#).
- [18] M. Del Zotto and G. Lockhart, “On Exceptional Instanton Strings,” [arXiv:1609.00310 \[hep-th\]](#).
- [19] J. Kim, K. Lee, and J. Park, “On elliptic genera of 6d string theories,” *JHEP* **10** (2018) 100, [arXiv:1801.01631 \[hep-th\]](#).
- [20] M. Del Zotto and G. Lockhart, “Universal Features of BPS Strings in Six-dimensional SCFTs,” *JHEP* **08** (2018) 173, [arXiv:1804.09694 \[hep-th\]](#).
- [21] S.-J. Lee, W. Lerche, and T. Weigand, “Tensionless Strings and the Weak Gravity Conjecture,” *JHEP* **10** (2018) 164, [arXiv:1808.05958 \[hep-th\]](#).
- [22] M.-x. Huang, S. Katz, and A. Klemm, “Topological String on elliptic CY 3-folds and the ring of Jacobi forms,” *JHEP* **10** (2015) 125, [arXiv:1501.04891 \[hep-th\]](#).
- [23] J. Gu, M.-x. Huang, A.-K. Kashani-Poor, and A. Klemm, “Refined BPS invariants of 6d SCFTs from anomalies and modularity,” *JHEP* **05** (2017) 130, [arXiv:1701.00764 \[hep-th\]](#).
- [24] M. Del Zotto, J. Gu, M.-X. Huang, A.-K. Kashani-Poor, A. Klemm, and G. Lockhart, “Topological Strings on Singular Elliptic Calabi-Yau 3-folds and Minimal 6d SCFTs,” *JHEP* **03** (2018) 156, [arXiv:1712.07017 \[hep-th\]](#).
- [25] C. F. Cota, A. Klemm, and T. Schimannek, “Topological strings on genus one fibered Calabi-Yau 3-folds and string dualities,” *JHEP* **11** (2019) 170, [arXiv:1910.01988 \[hep-th\]](#).
- [26] Z. Duan, J. Gu, and A.-K. Kashani-Poor, “Computing the elliptic genus of higher rank E-strings from genus 0 GW invariants,” *JHEP* **03** (2019) 078, [arXiv:1810.01280 \[hep-th\]](#).
- [27] P. Candelas, X. C. De La Ossa, P. S. Green, and L. Parkes, “A Pair of Calabi-Yau manifolds as an exactly soluble superconformal theory,” *Nucl. Phys.* **B359** (1991) 21–74. [AMS/IP Stud. Adv. Math.9,31(1998)].
- [28] S. Hosono, A. Klemm, S. Theisen, and S.-T. Yau, “Mirror symmetry, mirror map and applications to Calabi-Yau hypersurfaces,” *Commun. Math. Phys.* **167** (1995) 301–350, [arXiv:hep-th/9308122 \[hep-th\]](#).

- [29] V. Braun, “The Mori cone of a Calabi-Yau from toric Geometry,” *Masters Thesis, University of Texas at Austin* (1998) .
- [30] M. Del Zotto, J. J. Heckman, and D. R. Morrison, “6D SCFTs and Phases of 5D Theories,” *JHEP* **09** (2017) 147, [arXiv:1703.02981](https://arxiv.org/abs/1703.02981) [hep-th].
- [31] D. A. Cox, J. B. Little, and H. K. Schenck, *Toric varieties*, vol. 124 of *Graduate Studies in Mathematics*. American Mathematical Society, Providence, RI, 2011. <https://doi.org/10.1090/gsm/124>.
- [32] The Sage Developers, *SageMath, the Sage Mathematics Software System (Version 8.9)*, 2019. <https://www.sagemath.org>.
- [33] Wolfram Research Inc., *Mathematica, Version 12.0*. <https://www.wolfram.com/mathematica>. Champaign, IL, 2019.
- [34] R. Feger and T. W. Kephart, “LieART - A Mathematica application for Lie algebras and representation theory,” *Comput. Phys. Commun.* **192** (2015) 166–195, [arXiv:1206.6379](https://arxiv.org/abs/1206.6379) [math-ph].
- [35] P.-K. Oehlmann and T. Schimannek, “GV-Spectroscopy for F-theory on genus-one fibrations,” [arXiv:1912.09493](https://arxiv.org/abs/1912.09493) [hep-th].
- [36] S. H. Katz, D. R. Morrison, and M. R. Plesser, “Enhanced gauge symmetry in type II string theory,” *Nucl. Phys.* **B477** (1996) 105–140, [arXiv:hep-th/9601108](https://arxiv.org/abs/hep-th/9601108) [hep-th].
- [37] E. Witten, “Phase transitions in M theory and F theory,” *Nucl. Phys.* **B471** (1996) 195–216, [arXiv:hep-th/9603150](https://arxiv.org/abs/hep-th/9603150) [hep-th].
- [38] D. A. Cox, “The homogeneous coordinate ring of a toric variety,” *J. Algebraic Geom.* **4** no. 1, (1995) 17–50.
- [39] D. A. Cox, “Erratum to “The homogeneous coordinate ring of a toric variety”,” *J. Algebraic Geom.* **23** no. 2, (2014) 393–398. <https://doi.org/10.1090/S1056-3911-2013-00651-7>.
- [40] V. V. Batyrev, “Dual polyhedra and mirror symmetry for Calabi-Yau hypersurfaces in toric varieties,” *J. Alg. Geom.* **3** (1994) 493–545, [arXiv:alg-geom/9310003](https://arxiv.org/abs/alg-geom/9310003) [alg-geom].
- [41] V. V. Batyrev and L. A. Borisov, “On Calabi-Yau complete intersections in toric varieties,” [arXiv:alg-geom/9412017](https://arxiv.org/abs/alg-geom/9412017) [alg-geom].
- [42] D. A. Cox and S. Katz, *Mirror symmetry and algebraic geometry*, vol. 68 of *Mathematical Surveys and Monographs*. American Mathematical Society, Providence, RI, 1999. <https://doi.org/10.1090/surv/068>.

- [43] D. R. Morrison and W. Taylor, “Toric bases for 6D F-theory models,” *Fortsch. Phys.* **60** (2012) 1187–1216, [arXiv:1204.0283 \[hep-th\]](#).
- [44] K. A. Intriligator, D. R. Morrison, and N. Seiberg, “Five-dimensional supersymmetric gauge theories and degenerations of Calabi-Yau spaces,” *Nucl. Phys.* **B497** (1997) 56–100, [arXiv:hep-th/9702198 \[hep-th\]](#).
- [45] P. S. Aspinwall, S. H. Katz, and D. R. Morrison, “Lie groups, Calabi-Yau threefolds, and F theory,” *Adv. Theor. Math. Phys.* **4** (2000) 95–126, [arXiv:hep-th/0002012 \[hep-th\]](#).
- [46] D. S. Park, “Anomaly Equations and Intersection Theory,” *JHEP* **01** (2012) 093, [arXiv:1111.2351 \[hep-th\]](#).
- [47] E. Witten, “Mirror manifolds and topological field theory,” [arXiv:hep-th/9112056 \[hep-th\]](#). [AMS/IP Stud. Adv. Math.9,121(1998)].
- [48] M. Bershadsky, S. Cecotti, H. Ooguri, and C. Vafa, “Kodaira-Spencer theory of gravity and exact results for quantum string amplitudes,” *Commun. Math. Phys.* **165** (1994) 311–428, [arXiv:hep-th/9309140 \[hep-th\]](#).
- [49] R. L. Bryant and P. A. Griffiths, “Some observations on the infinitesimal period relations for regular threefolds with trivial canonical bundle,” in *Arithmetic and geometry, Vol. II*, vol. 36 of *Progr. Math.*, pp. 77–102. Birkhäuser Boston, Boston, MA, 1983.
- [50] S. Hosono, A. Klemm, S. Theisen, and S.-T. Yau, “Mirror symmetry, mirror map and applications to complete intersection Calabi-Yau spaces,” *Nucl. Phys.* **B433** (1995) 501–554, [arXiv:hep-th/9406055 \[hep-th\]](#). [AMS/IP Stud. Adv. Math.1,545(1996)].
- [51] V. V. Batyrev, “Variations of the mixed Hodge structure of affine hypersurfaces in algebraic tori,” *Duke Math. J.* **69** no. 2, (1993) 349–409. <https://doi.org/10.1215/S0012-7094-93-06917-7>.
- [52] D. R. Morrison, “Compactifications of moduli spaces inspired by mirror symmetry,” No. 218, pp. 243–271. 1993. Journées de Géométrie Algébrique d’Orsay (Orsay, 1992).
- [53] P. S. Aspinwall, B. R. Greene, and D. R. Morrison, “The Monomial divisor mirror map,” [arXiv:alg-geom/9309007 \[alg-geom\]](#).
- [54] P. Candelas, A. Font, S. H. Katz, and D. R. Morrison, “Mirror symmetry for two parameter models. 2.,” *Nucl. Phys.* **B429** (1994) 626–674, [arXiv:hep-th/9403187 \[hep-th\]](#).
- [55] E. Witten, “Quantum background independence in string theory,” in *Salamfest 1993:0257-275*, pp. 0257–275. 1993. [arXiv:hep-th/9306122 \[hep-th\]](#).

- [56] D. R. Morrison, “Beyond the Kähler cone,” in *Proceedings of the Hirzebruch 65 Conference on Algebraic Geometry (Ramat Gan, 1993)*, vol. 9 of *Israel Math. Conf. Proc.*, pp. 361–376. Bar-Ilan Univ., Ramat Gan, 1996.
- [57] A.-M. Li and Y. Ruan, “Symplectic surgery and Gromov-Witten invariants of Calabi-Yau 3-folds,” *Invent. Math.* **145** no. 1, (2001) 151–218.
<https://doi.org/10.1007/s002220100146>.